DRCEXC – a Collection of Benchmark Examples for Robust Control Design of Continuous-Time Dynamical Systems Version 1.0[1]

Da Wei Gu[2], Mihail M. Konstantinov[3], Volker Mehrmann[4], Petko H. Petkov[5], Hongguo Xu[6]

November 2002

[1]This paper describes Version 1.0 of the benchmark collection DRCEXC. It presents results of the European Community BRITE-EURAM III Thematic Networks Programme NICONET (contract number BRRT-CT97-5040) and is distributed by the Working Group on Software WGS. *WGS secretariat*: Mrs. Ida Tassens, ESAT - Katholieke Universiteit Leuven, Kasteelpark Arenberg 10, 3001 Leuven-Heverlee, BELGIUM. This report is also available by anonymous ftp from *wgs.esat.kuleuven.ac.be/pub/WGS/REPORTS/SLWN2002-8.ps.Z*

[2]Control Systems Research, Department of Engineering, University of Leicester, Leicester LE1 7RH, U.K. E-mail: `dag@le.ac.uk`

[3]Department of Mathematics, University of Architecture and Civil Engineering, 1 Hr. Smirnenski Blvd., 1421 Sofia, Bulgaria. E-mail: `mmk_fte@uacg.acad.bg`

[4]Institut für Mathematik MA 4-5, TU Berlin, Str. des 17. Juni, D-10623 Berlin, Germany. E-mail: `mehrmann@math.tu-berlin.de`

[5]Department of Automatics, TU Sofia, 1756 Sofia, Bulgaria. E-mail: `php@tu-sofia.acad.bg`

[6]Department of Mathematics, University of Kansas, Lawrence, KS 66045, USA. E-mail: `xu@math.ukans.edu`

Abstract

In this report we present a collection of benchmark example problems for robust control design of linear continuous-time systems. The collection is intended to be used with the *SLICOT* library of routines for $\mathcal{H}_\infty$ and μ-design of robust control systems. The present version of the collection includes nine systems. The benchmark examples are implemented in MATLAB M-files.

Key Words: Robust control systems design, $\mathcal{H}_\infty$ and μ-analysis and design, *SLICOT*

1 Introduction

In the analysis of numerical methods and their implementation as numerical software it is extremely important to test the correctness of the implementation as well as the performance of the method. This validation is one of the major steps in the construction of a software library, in particular, if this library is used in practical applications.

In order to carry out such tests it is necessary to have tools that yield an evaluation of the performance of the method as well as the implementation with respect to correctness, accuracy, and speed. Similar tools are needed to compare different numerical methods, to test their robustness, and also to analyze the behaviour of the methods in extreme situations, where the limit of the possible accuracy is reached.

In many application areas benchmark collections have been created that can partially serve for this purpose. Such collections are heavily used. In order to have a fair evaluation and a comparison of methods and software, there should be a standardized set of examples, which are freely available and on which newly developed methods and their implementations can be tested. Moreover, public benchmark collections can be used by developers of algorithms and software as a reference when reporting the results of numerical experiments in publications.

In order to make such collections useful it is important that they cover a wide range of problems. Two kinds of test problems are of particular interest. First, benchmark collections should contain so-called 'real world' examples, i.e., examples reflecting current problems in applications. Second, they must contain test examples which drive numerical methods and their implementations to a limit. These are ideal test cases because errors and failures usually occur only in extreme cases and these are often not covered by standard software validation procedures.

Unfortunately, up to now there is no available collection of benchmark examples for robust control design.

This is partly due to the fact that a formulation of a robust control problem is not unique, i.e., there are several factors which determine the augmented system description and which are subject to be set from the designer, namely the requirements imposed on the closed loop system in terms of robust stability and robust performance. The latter determine the partitioning of the augmented plant.

Unlike a formulation of a benchmark example for classical control problems, coining out a benchmark problem for robust control is a more complex task. It comprises

- generation of a *descriptor* state-space model of the nominal plant

$$\begin{aligned} E\dot{x}(t) &= Ax(t) + Bu(t) \\ y(t) &= Cx(t) + Du(t), \end{aligned} \tag{1}$$

  where $E, A \in \mathbb{R}^{n\times n}$, $B \in \mathbb{R}^{n\times m}$, $C \in \mathbb{R}^{p\times n}$, and $D \in \mathbb{R}^{p\times m}$. We refer to the vector-valued functions u, x, and y as the *input*, the *state*, and the *output* of the system, respectively.

  The descriptor system framework was chosen for the sake of generality and compatibility with contributions of such type of models. However, the current version of the collection contains *standard* systems, i.e., systems where $E = I_n$. Although there exists a well developed theory for descriptor systems including robust control issues, such examples are scarce in literature and tracking down reasonable descriptor benchmark examples is a hard problem.

- generation of a generalized (augmented) system P (Figure 1)

$$\begin{aligned} E\dot{x}(t) &= Ax(t) + B_1 w(t) + B_2 u(t), \\ z(t) &= C_1 x(t) + D_{11} w(t) + D_{12} u(t), \\ y(t) &= C_2 x(t) + D_{21} w(t) + D_{22} u(t), \end{aligned} \tag{2}$$

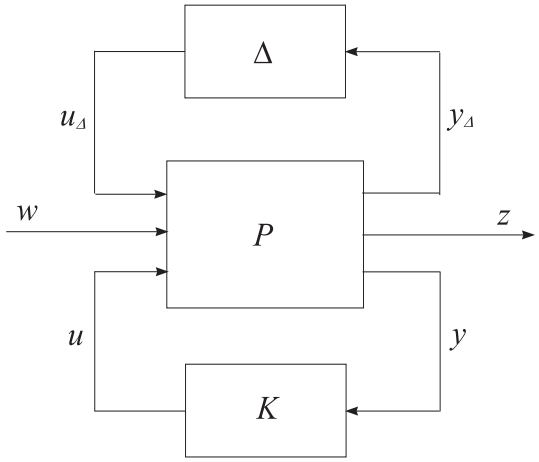

Figure 1: General robust control configuration

where $x(t)$ is the state vector, $w(t)$ the exogenous input vector, $u(t)$ the control input vector, $z(t)$ the error (controlled output) vector, and $y(t)$ the measurement vector. The choice of these vectors is subject to the design goal, the available information over the type and scale of uncertainties, the experience of the designer etc. That means that we provide one, sample representation of the generalized system. Every contributor is encouraged to include along with the standard state-space model, an augmented representation considered most acceptable. It should be accompanied by an explanation note specifying the choice of $z(t)$, $y(t)$, $u(t)$ and $w(t)$ and the particular design goals. Note that eventually the use of weighting (loop-shaping) functions should be taken into account in the generalized model. For instance, such functions arise in the S/KS mixed sensitivity $\mathcal{H}_\infty$ design. (See the transfer functions W_1 and W_2 in Figure 2). [13].

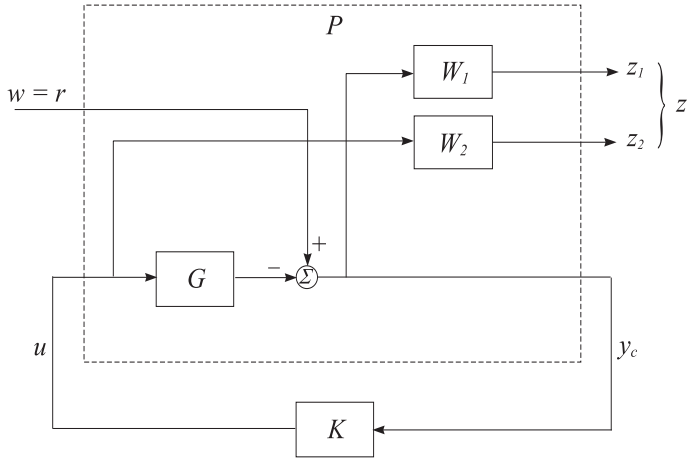

Figure 2: S/KS mixed sensitivity design

Nevertheless, the user of the collection has the freedom to change the generalized formulation according to his design needs having the nominal model (1).

Note also that in most of the cases especially when industrial examples are involved, the systems are strictly proper, i.e., there exists no direct link between the control input and the measurement output ($D_{22} = 0$).

- robust stability and performance specifications – in case of an industrial example they are provided from the manufacturer. If the latter are not driving the software 'to the limit' they may be set to be more rigid. The resulting controller will then ensure even larger robust stability and/or performance regions.

  Considering artificially created examples the appropriate specifications are usually derived via trial and error. As mentioned above these specifications determine the augmented structure.

A common procedure for robust control is the suboptimal solution of the optimal H_∞ problem which is formulated under the following typical set of assumptions [6, 17].

Assumptions:

A1 The pair (A, B_2) is *stabilizable* and the pair (A, C_2) is *detectible*.

A2 $D_{22} = 0$ and both D_{12} and D_{21} have full rank.

A3 The matrix $\left[\begin{smallmatrix} A-i\omega I & B_2 \\ C_1 & D_{12} \end{smallmatrix}\right]$ has full column rank for all real ω.

A4 The matrix $\left[\begin{smallmatrix} A-i\omega I & B_1 \\ C_2 & D_{21} \end{smallmatrix}\right]$ has full row rank for all real ω.

For the basic form of suboptimal H_∞ control, one introduces the two symmetric matrices

$$\begin{aligned} R_H(\gamma) &:= \begin{bmatrix} D_{11}^T \\ D_{12}^T \end{bmatrix} \begin{bmatrix} D_{11} & D_{12} \end{bmatrix} - \begin{bmatrix} \gamma^2 I_{m_1} & 0 \\ 0 & 0 \end{bmatrix}, \\ R_J(\gamma) &:= \begin{bmatrix} D_{11} \\ D_{21} \end{bmatrix} \begin{bmatrix} D_{11}^T & D_{21}^T \end{bmatrix} - \begin{bmatrix} \gamma^2 I_{p_1} & 0 \\ 0 & 0 \end{bmatrix}. \end{aligned} \tag{3}$$

We denote the largest γ for which any of the matrices $R_H(\gamma)$ and $R_J(\gamma)$ is singular by $\hat{\gamma}$. All numerical methods for the computation of a suboptimal H_∞ controller are essentially based on the following basic Theorem.

Theorem[17]. *Consider system (2) and R_H, R_J as in (3). Under assumptions A1–A4, there exists an internally stabilizing controller such that the transfer function from w to z satisfies $\|T_{zw}\|_\infty < \gamma$ if and only if the following four conditions hold.*

1. $\gamma > \hat{\gamma}$.

2. *There exists a positive semidefinite solution X_H of the algebraic Riccati equation associated with the Hamiltonian matrix*

$$\begin{aligned} H(\gamma) &= \begin{bmatrix} A_H(\gamma) & G_H(\gamma) \\ H_H(\gamma) & -A_H^T(\gamma) \end{bmatrix} \\ &= \begin{bmatrix} A & 0 \\ -C_1^T C_1 & -A^T \end{bmatrix} - \begin{bmatrix} B_1 & B_2 \\ -C_1^T D_{11} & -C_1^T D_{12} \end{bmatrix} R_H^{-1}(\gamma) \begin{bmatrix} D_{11}^T C_1 & B_1^T \\ D_{12}^T C_1 & B_2^T \end{bmatrix}. \end{aligned} \tag{4}$$

3. *There exists a positive semidefinite solution X_J of the algebraic Riccati equation associated with the Hamiltonian matrix*

$$J(\gamma) = \begin{bmatrix} A_J(\gamma) & G_J(\gamma) \\ H_J(\gamma) & -A_J^T(\gamma) \end{bmatrix} \tag{5}$$
$$= \begin{bmatrix} A^T & 0 \\ -B_1 B_1^T & -A \end{bmatrix} - \begin{bmatrix} C_1^T & C_2^T \\ -B_1 D_{11}^T & -B_1 D_{21}^T \end{bmatrix} R_J^{-1}(\gamma) \begin{bmatrix} D_{11} B_1^T & C_1 \\ D_{21}^T B_1^T & C_2 \end{bmatrix}.$$

4. *$\gamma^2 > \rho(X_H X_J)$ (where $\rho(X_H X_J)$ is the spectral radius ρ of $X_H X_J$).*

Numerical methods [6, 9, 12] essentially determine via an iterative procedure the largest γ where one of the conditions of this theorem fail. Some of the presented benchmark examples are devoted to situations where the conditions of Theorem 1 are difficult to check.

In the present collection it is assumed that an $\mathcal{H}_\infty$ optimization or μ design approach is to be applied to the examples. The output of the procedures consists of the standard systems representation, i.e., matrices E, A, B, C and D, as well as a sample default partitioning on the augmented plant A, B_1, B_2, C_1, C_2, D_{11}, D_{12}, D_{21} and D_{22}.

The examples in the collection are subdivided into four different *groups*:

- Group 1 — parameter-free problems of fixed size;
- Group 2 — parameter-dependent problems of fixed size;
- Group 3 — parameter-free examples of scalable size;
- Group 4 — parameter-dependent examples of scalable size.

In this version of the report we consider one example of a system from Group 1 and seven examples of systems from Group 2.

The examples in the Group 2 depend on several parameters, which have a direct impact on the algebraic properties of the systems.

The benchmark examples are implemented in MATLAB M-files, presented in the Appendix. The usage of the files requires implementation of the robust control toolbox [9] or the μ-toolbox [1].

The benchmark collection will be permanently updated and expanded. Suggestions and contributions to forthcoming releases will be highly appreciated.

2 Parameter-free problems of fixed size (Group 1)

The first example presents an 'academic' test problem.

Example 1.1 [8]

n	m	p
5	3	3

The system matrices are

$$E = I_5,\ A = \begin{bmatrix} 0 & 0 & 1.1320 & 0 & -1.0000 \\ 0 & -0.0538 & -0.1712 & 0 & 0.0705 \\ 0 & 0 & 0 & 1.0000 & 0 \\ 0 & 0.0485 & 0 & -0.8556 & -1.0130 \\ 0 & -0.2909 & 0 & 1.0532 & -0.6859 \end{bmatrix},$$

$$, B = \begin{bmatrix} 0 & 0 & 0 \\ -0.1200 & 1.0000 & 0 \\ 0 & 0 & 0 \\ 4.4190 & 0 & -1.6650 \\ 1.5750 & 0 & -0.0732 \end{bmatrix}, \; C = \begin{bmatrix} 1 & 0 & 0 & 0 & 0 \\ 0 & 1 & 0 & 0 & 0 \\ 0 & 0 & 1 & 0 & 0 \end{bmatrix}, \; D = 0_3$$

The design goal is to find a controller $u(t) = Ky(t)$ so that the closed-loop system satisfies the following requirements:

1. Robustness requirement: The maximum singular value of the complementary sensitivity matrix to lie below a line with a slope $-20\ dB/dec$ and for a frequency $100\ rad/s$ to have a value not bigger than $0\ dB$.
2. Performance requirement: To minimize the sensitivity function.

3 Parameter-dependent problems of fixed size (Group 2)

Example 2.1 [2]

n	m	p	parameter(s)	default value
2	3	3	α, β, δ, η, ϵ_1, ϵ_2	$\alpha = 1$, $\beta = 1$, $\delta = 1$, $\eta = 1$, $\epsilon_1 = \epsilon_2 = 0$.

The system matrices are

$$\begin{aligned} E &= I_2, \; A = \begin{bmatrix} -1 & 0 \\ 0 & -1 \end{bmatrix}, B = \begin{bmatrix} \epsilon_1 & 0 & 1 \\ 0 & \epsilon_2 & 1 \end{bmatrix} \\ C &= \begin{bmatrix} \alpha & 0 \\ 0 & \beta \\ \delta & \eta \end{bmatrix}, \; D = \begin{bmatrix} .5 & 0 & 0 \\ 0 & .5 & 1 \\ 0 & 1 & 0 \end{bmatrix} \end{aligned}$$

Here the Hamiltonian $H(\gamma)$ in Theorem 1 has eigenvalues ± 1 and $\pm\sqrt{(1+\eta)^2+\alpha^2}$ and the positive semidefinite Riccati solution corresponding to $H(\gamma)$ is

$$\begin{aligned} X_H &= \frac{\alpha^2\eta(2+\eta)}{(1-\frac{1}{4}\gamma^{-2})(2\eta+\eta^2+\alpha^2)} \\ &\times \begin{bmatrix} \frac{1}{2} + \frac{\alpha^2}{\eta(2+\eta)(1+\sqrt{(1+\eta)^2+\alpha^2})} & \frac{1}{1+\sqrt{(1+\eta)^2+\alpha^2}} - \frac{1}{2} \\ \frac{1}{1+\sqrt{(1+\eta)^2+\alpha^2}} - \frac{1}{2} & \eta\left(\frac{1}{2(2+\eta)} - \frac{1}{(1+\sqrt{(1+\eta)^2+\alpha^2})(1+\eta+\sqrt{(1+\eta)^2+\alpha^2})}\right) \end{bmatrix}, \end{aligned}$$

and the stable Riccati solution corresponding to the other Hamiltonian $J(\gamma)$ is always $X_J = 0$. The suboptimal γ according to Theorem 1 is $\gamma_{subopt} = \frac{1}{2}$ For $\gamma \to \gamma_{subopt}$ the Riccati solution X_H converges to infinity, and the Hamiltonian matrix $H(\gamma)$ becomes ill-defined. Furthermore, the fourth condition in Theorem 1 never fails, because $\rho(X_J X_H) = 0$ for all $\gamma > \gamma_{opt}$.

Example 2.2 [17]

n	m	p	parameter(s)	default value
5	2	2	α	$\alpha = 10^{-10}$.

The system matrices are

$$A = \begin{bmatrix} -\alpha & 0 & 1 & -2 & 1 \\ 0 & -100 & 0 & 0 & 0 \\ 0 & 0 & 0 & -2\alpha & \alpha \\ 0 & 0 & 0 & 0 & 1 \\ 0 & 0 & 0 & 3 & 2 \end{bmatrix}, \; B = \begin{bmatrix} 1 & 0 \\ 0 & -90 \\ \alpha & 0 \\ 0 & 0 \\ 0 & 0 \end{bmatrix},$$

$$C = \begin{bmatrix} 1 & 0 & 0 & 0 & 0 \\ 0 & 1 & 0 & 0 & 0 \\ 0 & 0 & 1 & -2 & 1 \end{bmatrix}, \; D = \begin{bmatrix} 0 & 0 \\ 0 & 1 \\ 1 & 0 \end{bmatrix}.$$

we have $\gamma_{subopt} \approx 7.854$ *independent of the choice of* α*. Choosing* α *close to or on the imaginary axis makes the problem very difficult to solve numerically.*

Example 2.3 [2]

n	m	p	parameter(s)	default value
2	3	3	α	$\alpha = 3.$

The system matrices are

$$A = \begin{bmatrix} 2 & -1 \\ 0 & -1 \end{bmatrix}, \; B = \begin{bmatrix} 0 & 1 & -1 \\ 0 & 1 & -2 \end{bmatrix},$$
$$C = \begin{bmatrix} 1 & 0 \\ 0 & 1 \\ 4 & -2 \end{bmatrix}, \; D = \begin{bmatrix} \alpha & 0 & 0 \\ 0 & -1 & 1 \\ 0 & 1 & 0 \end{bmatrix}.$$

we have actually the optimal $\gamma_{opt} \approx 0.7279748414803329$ *independent of the choice of* α*.*

Here in the neighborhood of γ_{opt} *the Riccati solutions are positive definite and the system is stabilized. No eigenvalues are near the imaginary axis. Most numerical methods except for [2] are only able to find* $\gamma_{subopt} = \alpha$*.*

Example 2.4 Mass/damper/spring system [17] (see also [1])

n	m	p	parameter(s)	default value
2	1	1	m, c, k	$\bar{m} = 3$, $\bar{c} = 1$, $k = 2$

This benchmark example problem is a second-order system representing a single degree-of-freedom mass-damper-spring system (Figure 3) with uncertain parameters:

$$m\ddot{x} + c\dot{x} + kx = u,$$

where x is the position of the mass and $u = F$ is the force acting on the mass.

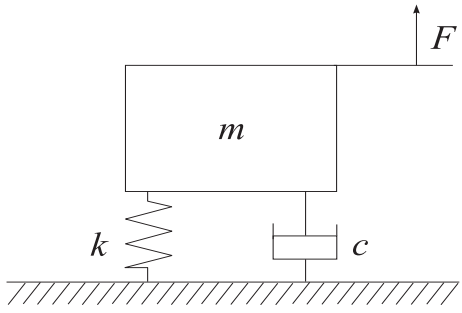

Figure 3: Mass-damper-spring system with uncertain parameters

The uncertain parameters m, c and k lie in the following intervals

$$m = \bar{m}\,(1 + 0.4\delta_m)\,, \; c = \bar{c}\,(1 + 0.2\delta_c)\,, \; k = \bar{k}\,(1 + 0.3\delta_k)\,,$$

where $-1 \leq \delta_m,\, \delta_c,\, \delta_k \leq 1$

The block diagram for the system is shown in Figure 4. As usual a parameter uncertainty model is

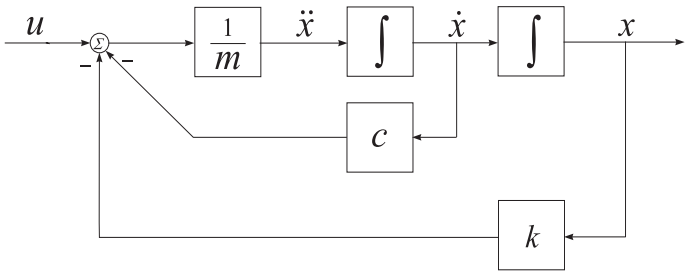

Figure 4: Second order mass-damper-spring system

derived by using lower/upper linear fractional transformations (LFT) of the varying parameters.

For the sake of generality we redefine the uncertainty intervals as

$$m = \bar{m}\,(1 + p_m \delta_m)\,,\ c = \bar{c}\,(1 + p_c \delta_c)\,,\ k = \bar{k}\,(1 + p_k \delta_k)\,,$$

where p_m, p_c, p_k are the relative changes in m, c and k, respectively. The quantity $\frac{1}{m}$ is represented as an upper linear fractional transformation (LFT) in δ_m:

$$\frac{1}{m} = \frac{1}{\bar{m}\,(1 + p_m \delta_m)} = \frac{1}{\bar{m}} - \frac{p_m}{\bar{m}} \delta_m\,(1 + p_m \delta_m)^{-1} = F_U\,(M_m,\, \delta_m)$$

with

$$M_m = \begin{bmatrix} -p_m & \frac{1}{\bar{m}} \\ -p_m & \frac{1}{\bar{m}} \end{bmatrix}.$$

Parameters c and k are also represented as upper LFT's in δ_c and δ_k, respectively in the same fashion:

$$c = F_U\,(M_c,\, \delta_c) \quad \text{with} \quad M_c = \begin{bmatrix} 0 & \bar{c} \\ p_c & \bar{c} \end{bmatrix},$$

$$k = F_U\,(M_k,\, \delta_k) \quad \text{with} \quad M_k = \begin{bmatrix} 0 & \bar{k} \\ p_k & \bar{k} \end{bmatrix}.$$

The LFT representation of the model is performed to isolate the uncertain parameters δ_m, δ_c and δ_k as shown in Figure 5. The system equations are

$$\left[\begin{array}{c} \dot{x}_1 \\ \dot{x}_2 \\ \hline y_m \\ y_c \\ y_k \\ \hline y \end{array}\right] = \left[\begin{array}{c|c|c} A & B_1 & B_2 \\ \hline C_1 & D_{11} & D_{12} \\ \hline C_2 & D_{21} & D_{22} \end{array}\right] \left[\begin{array}{c} x_1 \\ x_2 \\ \hline u_m \\ u_c \\ u_k \\ \hline u \end{array}\right],$$

$$\left[\begin{array}{c} u_m \\ u_c \\ u_k \end{array}\right] = \left[\begin{array}{ccc} \delta_m & 0 & 0 \\ 0 & \delta_c & 0 \\ 0 & 0 & \delta_k \end{array}\right] \left[\begin{array}{c} y_m \\ y_c \\ y_k \end{array}\right],$$

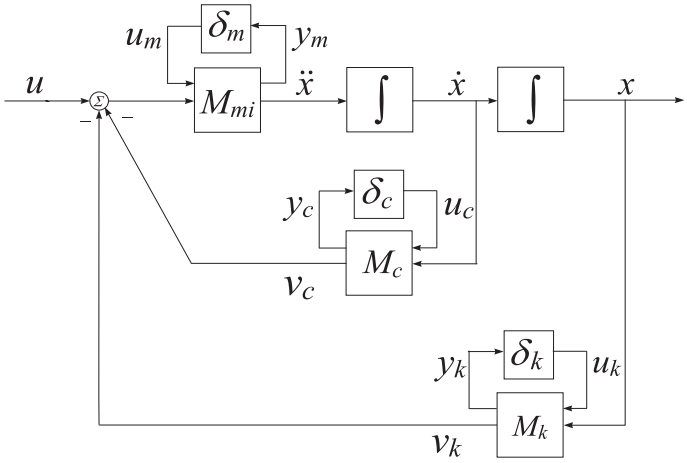

Figure 5: Block diagram of the system with uncertain parameters

where

$$A = \begin{bmatrix} 0 & 1 \\ -\frac{\bar{k}}{\bar{m}} & -\frac{\bar{c}}{\bar{m}} \end{bmatrix}, \qquad B_1 = \begin{bmatrix} 0 & 0 & 0 \\ -p_m & -\frac{p_c}{\bar{m}} & -\frac{p_k}{\bar{m}} \end{bmatrix}, \qquad B_2 = \begin{bmatrix} 0 \\ \frac{1}{\bar{m}} \end{bmatrix},$$

$$C_1 = \begin{bmatrix} -\frac{\bar{k}}{\bar{m}} & -\frac{\bar{c}}{\bar{m}} \\ 0 & \bar{c} \\ \bar{k} & 0 \end{bmatrix}, \quad D_{11} = \begin{bmatrix} -p_m & -\frac{p_c}{\bar{m}} & -\frac{p_k}{\bar{m}} \\ 0 & 0 & 0 \\ 0 & 0 & 0 \end{bmatrix}, \quad D_{12} = \begin{bmatrix} \frac{1}{\bar{m}} \\ 0 \\ 0 \end{bmatrix},$$

$$C_2 = \begin{bmatrix} 1 & 0 \end{bmatrix}, \qquad D_{21} = \begin{bmatrix} 0 & 0 & 0 \end{bmatrix}, \qquad D_{22} = 0.$$

Thus, the uncertain behaviour of the original system is described by the upper LFT

$$y = F_U(G, \Delta)\, u,$$

with

$$G = \left[\begin{array}{c|cc} A & B_1 & B_2 \\ \hline C_1 & D_{11} & D_{12} \\ C_2 & D_{21} & D_{22} \end{array}\right], \; \Delta = \begin{bmatrix} \delta_m & 0 & 0 \\ 0 & \delta_c & 0 \\ 0 & 0 & \delta_k \end{bmatrix}.$$

The Bode plots of the perturbed system for $\bar{m} = 3,\ \bar{c} = 1,\ \bar{k} = 2,\ p_m = 0.4,\ p_c = 0.2,\ p_k = 0.3$ and $-1 \le \delta_m,\ \delta_c,\ \delta_k \le 1$ are shown in Figure 6.

Design Goals

Find a linear feedback controller $u(s) = K(s)y(s)$ with the following properties:

- Nominal performance – for a unit step reference signal the controlled output has a settling time of 10 seconds and overshoot less or equal than 20%. The nominal system is $\bar{m} = 3$, $\bar{c} = 1$, $\bar{k} = 2$.
- Robust stability – the closed-loop system is stable for $1.8 \le m \le 4.2$, $0.8 \le c \le 1.2$, $1.4 \le k \le 2.6$.
- Robustness is achieved with "reasonable" bandwidth and control effort, (e.g. peak control input).
- "Reasonable" controller order – The order of the controller is not too large.

Example 2.5 Two-mass-spring system [15] (see also [16])

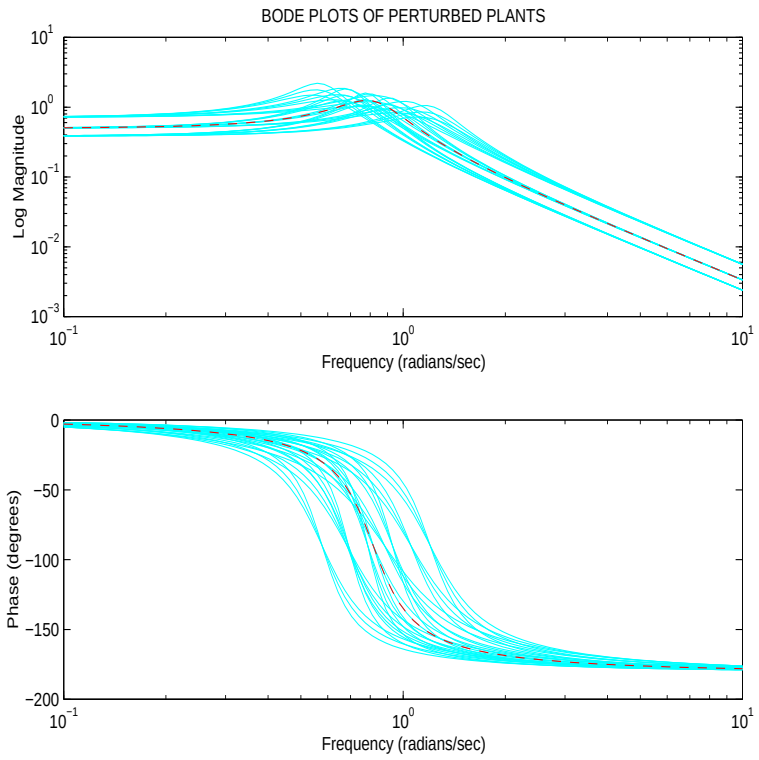

Figure 6: Bode plots of the perturbed open-loop system

n	m	p	parameter(s)	default value
4	1	1	m_1, m_2, k	$\bar{m}_1 = \bar{m}_2 = 1$, $k = 1.25$

This benchmark example problem represents a two-mass-spring system shown in figure 7. The system

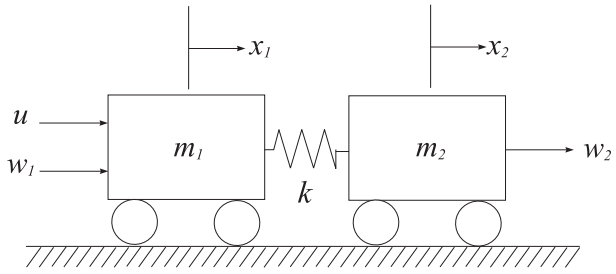

Figure 7: Two-mass-spring system

is described by two coupled second-order differential equations

$$\begin{array}{lcl} m_1\ddot{x} & = & -k\,(x_1 - x_2) + u + w_1, \\ m_2\ddot{x}_2 & = & k\,(x_1 - x_2) + w_2, \\ y & = & x_2 + v, \\ z & = & x_2, \\ v & = & W_n\ n, \end{array}$$

where x_1 and x_2 are the positions of body 1 and body 2, respectively, u is the control input acting on body 1, w_1 and w_2 represent the plant disturbances acting on body 1 and body 2, respectively, y is the sensor output, v is the sensor noise with a spectrum modelled by a filter W_n (n is white noise) and z is the output to be controlled (performance variable).

The system can be represented in state-space form as:

$$\begin{bmatrix} \dot{x}_1 \\ \dot{x}_2 \\ \dot{x}_3, \\ \dot{x}_4 \end{bmatrix} = \begin{bmatrix} 0 & 0 & 1 & 0 \\ 0 & 0 & 0 & 1 \\ -k/m_1 & k/m_1 & 0 & 0 \\ k/m_2 & -k/m_2 & 0 & 0 \end{bmatrix} \begin{bmatrix} x_1 \\ x_2 \\ x_3 \\ x_4 \end{bmatrix} + \begin{bmatrix} 0 \\ 0 \\ 1/m_1 \\ 0 \end{bmatrix} (u + w_1) + \begin{bmatrix} 0 \\ 0 \\ 0 \\ 1/m_2 \end{bmatrix} w_2,$$

where $x_3 = \dot{x}_1$ and $x_4 = \dot{x}_2$ are the velocities of body 1 and body 2, respectively.

A block diagram of the system is shown in Figure 8. The uncertain parameters m_1, m_2 and k are

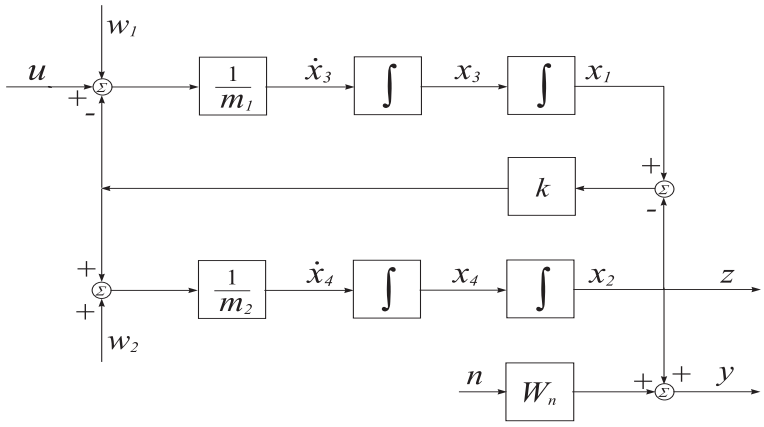

Figure 8: Block diagram of the two-mass-spring system

represented as

$$m_1 = \bar{m}_1\,(1 + p_{m_1}\delta_{m_1})\,,\ m_2 = \bar{m}_2\,(1 + p_{m_2}\delta_{m_2})\,,\ k = \bar{k}\,(1 + p_k\delta_k)\,,$$

where p_{m_1}, p_{m_2}, p_k are the relative changes in m_1, m_2 and k, respectively, and $-1 \le \delta_{m_1}, \delta_{m_2}, \delta_k \le 1$.

The quantities $\frac{1}{m_1}$ and $\frac{1}{m_2}$ may be represented as lower LFT in δ_{m_1}, δ_{m_2}, respectively:

$$\frac{1}{m_1} = F_L\,(M_{m_1},\, \delta_{m_1})\,,\ \ \frac{1}{m_2} = F_L\,(M_{m_2},\, \delta_{m_2})\,,$$

with

$$M_{m_1} = \begin{bmatrix} 1/\bar{m}_1 & -p_{m_1} \\ 1/\bar{m}_1 & -p_{m_1} \end{bmatrix},\ \ M_{m_2} = \begin{bmatrix} 1/\bar{m}_2 & -p_{m_2} \\ 1/\bar{m}_2 & -p_{m_2} \end{bmatrix}.$$

The parameter k may be represented as a lower LFT in δ_k

$$k = F_L\,(M_k,\, \delta_k)$$

with

$$M_k = \begin{bmatrix} \bar{k} & p_k \\ \bar{k} & 0 \end{bmatrix}.$$

Denoting the inputs and outputs of the uncertain parameters δ_{m_1}, δ_{m_2} and δ_k as y_{m_1}, y_{m_2}, y_k and u_{m_1}, u_{m_2}, u_k, respectively, the latter can be isolated as shown in Figure 9. The system equations are

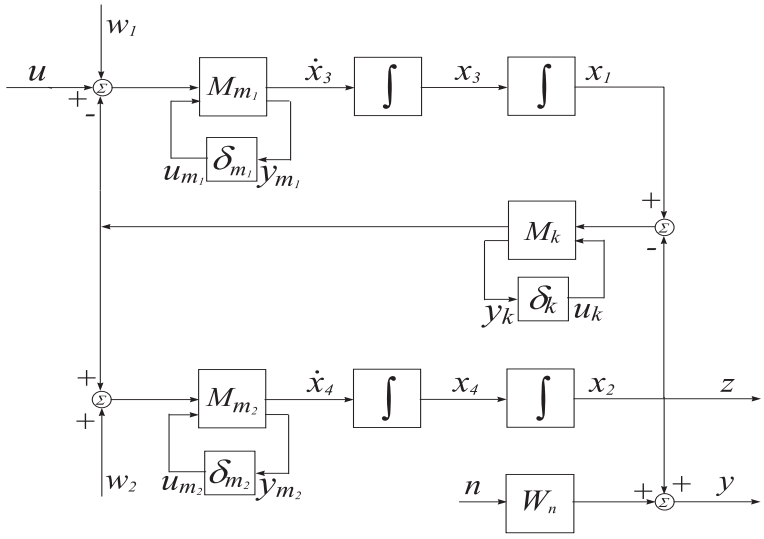

Figure 9: Block diagram of the two-mass-spring system with uncertain parameters

$$\left[\begin{array}{c} \dot{x}_1 \\ \dot{x}_2 \\ \dot{x}_3 \\ \dot{x}_4 \\ \hline y_k \\ y_{m_1} \\ y_{m_2} \\ \hline z \end{array}\right] = \left[\begin{array}{c|c|c} & & \\ A & B_1 & B_2 \\ & & \\ \hline & & \\ C_1 & D_{11} & D_{12} \\ & & \\ \hline & & \\ C_2 & D_{21} & D_{22} \\ & & \end{array}\right] \left[\begin{array}{c} x_1 \\ x_2 \\ x_3 \\ x_4 \\ \hline u_k \\ u_{m_1} \\ u_{m_2} \\ \hline w_1 \\ w_2 \\ u \end{array}\right],$$

$$\begin{bmatrix} u_k \\ u_{m_1} \\ u_{m_2} \end{bmatrix} = \begin{bmatrix} \delta_k & 0 & 0 \\ 0 & \delta_{m_1} & 0 \\ 0 & 0 & \delta_{m_2} \end{bmatrix} \begin{bmatrix} y_k \\ y_{m_1} \\ y_{m_2} \end{bmatrix},$$

with

$$A = \begin{bmatrix} 0 & 0 & 1 & 0 \\ 0 & 0 & 0 & 1 \\ -\bar{k}/\bar{m}_1 & \bar{k}/\bar{m}_1 & 0 & 0 \\ \bar{k}/\bar{m}_2 & -\bar{k}/\bar{m}_2 & 0 & 0 \end{bmatrix}, \quad B_1 = \begin{bmatrix} 0 & 0 & 0 \\ 0 & 0 & 0 \\ -p_k/\bar{m}_1 & -p_{m_1} & 0 \\ p_k/\bar{m}_2 & 0 & -p_{m_2} \end{bmatrix}, \quad B_2 = \begin{bmatrix} 0 & 0 & 0 \\ 0 & 0 & 0 \\ 1/\bar{m}_1 & 0 & 1/\bar{m}_1 \\ 0 & 1/\bar{m}_2 & 0 \end{bmatrix},$$

$$C_1 = \begin{bmatrix} \bar{k} & -\bar{k} & 0 & 0 \\ -\bar{k}/m_1 & \bar{k}/m_1 & 0 & 0 \\ \bar{k}/m_2 & -\bar{k}/m_2 & 0 & 0 \end{bmatrix}, \quad D_{11} = \begin{bmatrix} 0 & 0 & 0 \\ -p_k/\bar{m}_1 & -p_{m_1} & 0 \\ p_k/\bar{m}_2 & 0 & -p_{m_2} \end{bmatrix}, \quad D_{12} = \begin{bmatrix} 0 & 0 & 0 \\ 1/\bar{m}_1 & 0 & 1/\bar{m}_1 \\ 0 & 1/\bar{m}_2 & 0 \end{bmatrix},$$

$$C_2 = [\,0 \quad 1 \quad 0 \quad 0\,], \qquad D_{21} = [\,0 \quad 0 \quad 0\,], \qquad D_{22} = [\,0 \quad 0 \quad 0\,].$$

The uncertain behaviour of the original system is described by the upper LFT

$$z = F_U\,(G,\,\Delta) \begin{bmatrix} w_1 \\ w_2 \\ u \end{bmatrix},$$

with

$$G = \left[\begin{array}{c|cc} A & B_1 & B_2 \\ \hline C_1 & D_{11} & D_{12} \\ C_2 & D_{21} & D_{22} \end{array}\right], \; \Delta = \begin{bmatrix} \delta_k & 0 & 0 \\ 0 & \delta_{m_1} & 0 \\ 0 & 0 & \delta_{m_2} \end{bmatrix}.$$

The Bode plots of the perturbed system for $\bar{m}_1 = \bar{m}_2 = 1$, $\bar{k} = 1.25$, $p_{m_1} = p_{m_2} = 0.1$, $p_k = 0.24$ and $-1 \leq \delta_{m_1}, \delta_{m_2}, \delta_k \leq 1$ are shown in Figure 10.

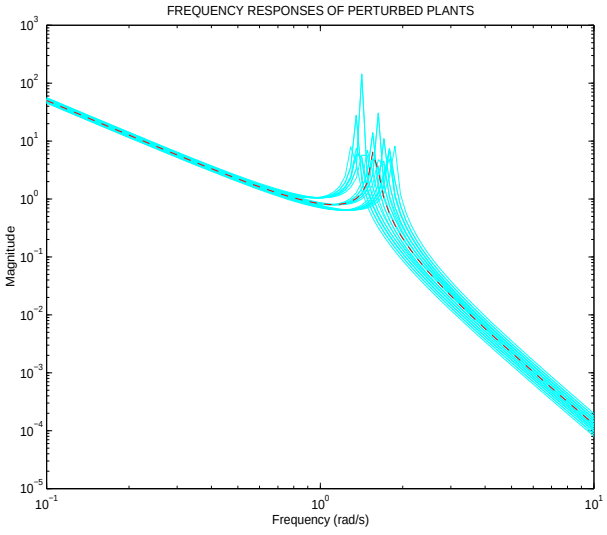

Figure 10: Bode plots of the perturbed open-loop system

Design Goal

Determine a linear feedback controller $u(s) = K(s)y(s)$ with the following properties:

- Nominal performance – for a unit step reference signal the controlled output z has a settling time of 20 seconds and overshoot less or equal than 30%. The nominal system is $\bar{m}_1 = 1$, $\bar{m}_2 = 1$, $\bar{k} = 1.25$.

- Robust stability – the closed-loop system is stable for $0.9 \leq m_1 \leq 1.1$, $0.9 \leq m_2 \leq 1.1$, $0.95 \leq k \leq 1.55$.
- The closed-loop system is insensitive to high-frequency noise.
- Robustness is achieved with "reasonable" bandwidth and control effort, (e.g. peak control input)
- "Reasonable" controller order – The order of the controller is not too large.

Example 2.6 The IFAC 93 benchmark problem [14].

n	m	p	parameter(s)	default value
7	1	1	T_1, T_2, ω_0, ξ, K	randomly assigned

This example models one of the loops in an Australian company which is a time-varying single-input single-output process. Depending on production conditions, the loop operates at three different stress levels with higher stress levels inducing larger time variations. The set-point of the loop is a square wave varying between $+1$ and -1 with a period 20 seconds.

The model is given by the following transfer function

$$G(s) = \frac{K(-T_2 s+1)\omega_0^2}{\left(s^2+2\zeta\omega_0 s+\omega_0^2\right)(T_1 s+1)} \times \frac{\omega_\delta^2}{\left(s^2+2\zeta_\delta\omega_\delta s+\omega_\delta^2\right)\left(T_1^\delta s+1\right)\left(T_2^\delta s+1\right)}\,. \tag{6}$$

The high-frequency dynamics is fixed in time and for all stress levels (levels of uncertainty of the parameters):

$$T_1^\delta = 1/8\,, \quad T_2^\delta = 1/12, \quad \omega_\delta = 15, \quad \zeta_\delta = 0.6\,.$$

The dominant dynamics has, at all stress levels, the nominal values:

$$T_1 = 5, \quad T_2 = 0.4, \quad \omega_0 = 5, \quad \zeta = 0.3, \quad K = 1\,.$$

The variations around the nominal values are as follows:

Stress Level 1: $T_1 = 5 \pm 0.2$, $T_2 = 0.4 \pm 0.05$, $\omega_0 = 5 \pm 1.5$, $\xi = 0.3 \pm 0.1$, $K = 1$.

Stress Level 2: $T_1 = 5 \pm 0.3$, $T_2 = 0.4 \pm 0.1$, $\omega_0 = 5 \pm 2.5$, $\xi = 0.3 \pm 0.15$, $K = 1 \pm 0.15$.

Stress Level 3: $T_1 = 5 \pm 0.3$, $T_2 = 0.4 \pm 0.15$, $\omega_0 = 5 \pm 3$, $\xi = 0.3 \pm 0.15$, $K = 1 \pm 0.5$.

Similarly to the preceding two examples the parameter uncertainty model of the part of the model representing the dominant dynamics is derived using LFT's of the varying parameters.

The uncertainty parameters are

$$K = \bar{K}\left(1 + p_K\delta_K\right), \;\; \omega_0 = \bar{\omega}\left(1 + p_\omega\delta_\omega\right), \;\; \xi = \bar{\xi}\left(1 + p_\xi\delta_\xi\right), \;\; T_1 = \bar{T}_1\left(1 + p_{T_1}\delta_{T_1}\right), \;\; T_2 = \bar{T}_2\left(1 + p_{T_2}\delta_{T_2}\right).$$

Parameters K, ω_0, ξ and T_2 are represented as upper LFT's in δ_K, δ_ω, δ_ξ and δ_{T_2}, respectively, in the same fashion:

$$K = F_U\left(M_K, \delta_K\right) \quad \text{with} \quad M_K = \begin{bmatrix} 0 & \bar{K} \\ p_K & \bar{K} \end{bmatrix},$$

$$\omega_0 = F_U\left(M_\omega, \delta_\omega\right) \quad \text{with} \quad M_\omega = \begin{bmatrix} 0 & \bar{\omega} \\ p_\omega & \bar{\omega} \end{bmatrix},$$

$$\xi = F_U\left(M_\xi, \delta_\xi\right) \quad \text{with} \quad M_\xi = \begin{bmatrix} 0 & \bar{\xi} \\ p_\xi & \bar{\xi} \end{bmatrix},$$

$$T_2 = F_U\left(M_{T_2}, \delta_{T_2}\right) \quad \text{with} \quad M_{T_2} = \begin{bmatrix} 0 & \bar{T}_2 \\ p_{T_2} & \bar{T}_2 \end{bmatrix}.$$

The quantity $\frac{1}{T_1}$ is represented by an upper LFT in δ_{T_1}

$$\frac{1}{T_1} = \frac{1}{\bar{T}_1} - \frac{p_{T_1}}{\bar{T}_1}\delta_{T_1}\left(1 + p_{T_1}\delta_{T_1}\right)^{-1} = F_U\left(M_{T_1},\, \delta_{T_1}\right),$$

with

$$M_{T_1} = \begin{bmatrix} -p_{T_1} & 1/\bar{T}_1 \\ -p_{T_1} & 1/\bar{T}_1 \end{bmatrix}.$$

The block-diagram of the system with uncertain parameters is shown in Figure 11. The uncertain

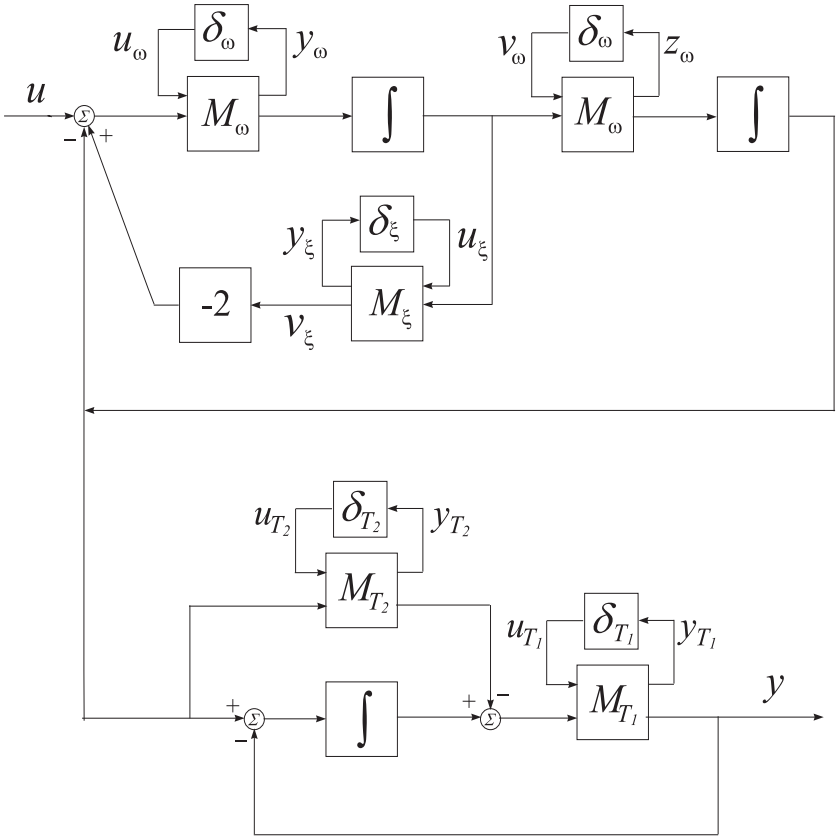

Figure 11: Block-diagram of the IFAC 93 benchmark example system with uncertain parameters

behaviour of the original system is described by the upper LFT

$$y = F_U\left(G,\, \Delta\right) u$$

with

$$\Delta = \begin{bmatrix} \delta_K & 0 & 0 & 0 & 0 & 0 \\ 0 & \delta_\omega & 0 & 0 & 0 & 0 \\ 0 & 0 & \delta_\omega & 0 & 0 & 0 \\ 0 & 0 & 0 & \delta_\xi & 0 & 0 \\ 0 & 0 & 0 & 0 & \delta_{T_1} & 0 \\ 0 & 0 & 0 & 0 & 0 & \delta_{T_2} \end{bmatrix}.$$

Note that the uncertainty δ_ω is repeated twice.

The matrix G can easily be obtained by using the function `sysic` from μ-toolbox, as shown in the file `mod_ifac`, given in the Appendix.

Design Goals

For each stress level, design a controller to achieve as fast a rise time as possible, subject to the following conditions:

- The plant output must be within -1.5 and $+1.5$ at all times.
- Zero steady state tracking error (modulo high frequency noise).
- It is preferable if under/overshoot is around 0.2 most of the time (occasional large over/undershoots are acceptable as long as the output is within ± 1.5).
- Small settling time.
- Plant input saturates at -5.0 and $+5.0$.

Example 2.7 Triple inverted pendulum system [4] (see also [10])

n	m	p
10	2	3

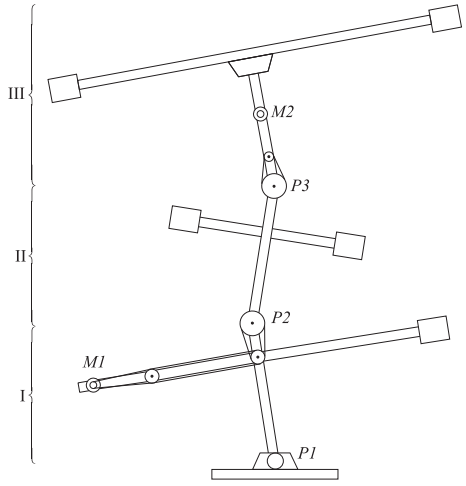

Figure 12: Triple inverted pendulum

The triple inverted pendulum is considered in the form of the experimental setup shown in Figure 12. The pendulum consists of three arms which are hinged by ball bearings and can rotate in the vertical plane. The torques of two upper hinges are controlled with the lowest hinge made free for rotation. By controlling the angles of the two upper arms around the specified values, the pendulum can be stabilized inversely with the desired angle attitudes. A horizontal bar is fixed to each of the arms to ease the control by increasing the moment of inertia. Two DC motors, M_1 and M_2, are mounted on the first and third arm, respectively, acting as actuators which provide torques to the two upper hinges through timing belts. The potentiometers P_1, P_2 and P_3 are fixed to the hinges to measure the corresponding angles. Let Θ_i denote the angle of the i-th arm. The first potentiometer measures the angle Θ_1, and the second and third potentiometers measure the angles $\Theta_2 - \Theta_1$ and $\Theta_3 - \Theta_2$, respectively (Figure 13).

The mathematical description of the triple inverted pendulum is derived under the following assumptions:

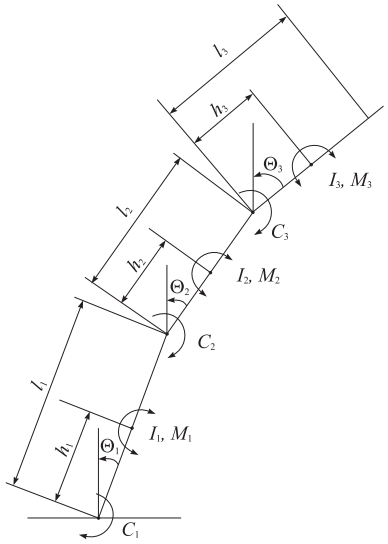

Figure 13: Geometric relationships for the triple inverted pendulum

a) each arm is a rigid body;

b) the lengths of the belts remain constant during the work of the system;

c) the friction force in the bottom hinge is proportional to the velocity of the bottom arm and the friction forces in the upper hinges are proportional to the differences of the respective velocities of two neighbouring arms.

First we consider the mathematical description of the pendulum itself without the actuators. The pendulum model is constructed using the Lagrange differential equations [4]. After linearization of these equations under the assumption of small deviations of the pendulum from the vertical position one obtains the vector-matrix equation

$$M \begin{bmatrix} \ddot{\Theta}_1 \\ \ddot{\Theta}_2 \\ \ddot{\Theta}_3 \end{bmatrix} + N \begin{bmatrix} \dot{\Theta}_1 \\ \dot{\Theta}_2 \\ \dot{\Theta}_3 \end{bmatrix} + P \begin{bmatrix} \Theta_1 \\ \Theta_2 \\ \Theta_3 \end{bmatrix} + G \begin{bmatrix} t_{m_1} \\ t_{m_2} \end{bmatrix} = 0, \tag{7}$$

where

$$M = \begin{bmatrix} J_1 + I_{p_1} & l_1 M_2 - I_{p_1} & l_1 M_3 \\ l_1 M_2 - I_{p_1} & J_2 + I_{p_1} + I_{p_2} & l_2 M_3 - I_{p_2} \\ l_1 M_3 & l_2 M_3 - I_{p_2} & J_3 + I_{p_2} \end{bmatrix},$$

$$N = \begin{bmatrix} C_1 + C_2 + C_{p_1} & -C_2 - C_{p_1} & 0 \\ -C_2 - C_{p_1} & C_{p_1} + C_{p_2} + C_2 + C_3 & -C_3 - C_{p_2} \\ 0 & -C_3 - C_{p_2} & C_3 + C_{p_2} \end{bmatrix},$$

$$P = \begin{bmatrix} M_1 g & 0 & 0 \\ 0 & -M_2 g & 0 \\ 0 & 0 & -M_3 g \end{bmatrix}, \; G = \begin{bmatrix} K_1 & 0 \\ -K_1 & K_2 \\ 0 & -K_2 \end{bmatrix},$$

$$C_{p_i} = C_{p_i'} + K_i^2 C_{m_i}, \; I_{p_i} = I_{p_i'} + K_i^2 I_{m_i},$$

$$M_1 = m_1 h_1 + m_2 l_1 + m_3 l_1, \; M_2 = m_2 h_2 + m_3 l_2, \; M_3 = m_3 h_3,$$

Table 1: System nomenclature

Symbol	Description
u_j	input voltage to the j-th motor
t_{m_j}	control torque of the j-th motor
l_i	length of the i-th arm
h_i	the distance from the bottom to the center of gravity of i-th arm
m_i	mass of the i-th arm
I_i	moment of inertia of i-th arm around the center of gravity
C_i	coefficient of viscous friction of i-th hinge
Θ_i	angle of i-th arm from vertical line
C_{m_i}	coefficient of viscous friction of i-th motor
I_{m_i}	moment of inertia of i-th motor
K_i	ratio of teeth of belt-pulley system of i-th hinge
$C_{p_i'}$	coefficient of viscous friction of belt-pulley system of i-th hinge
$I_{p_i'}$	moment of inertia of belt-pulley system of i-th hinge
α_i	gain of the i-th potentiometer
g	acceleration of gravity

$$J_1 = I_1 + m_1 h_1^2 + m_2 l_1^2 + m_3 l_1^2,\ J_2 = I_2 + m_2 h_2^2 + m_3 l_2^2,$$
$$J_3 = I_3 + m_3 h_3^2,$$

and all the other parameters and variables are defined in Table 1.

By introducing the control torques vector $t_m = [t_{m_1}\ t_{m_2}]^T$ and denoting $\Theta = [\Theta_1\ \Theta_2\ \Theta_3]^T$, the equation (7) can be written in the form

$$M\ddot{\Theta} + N\dot{\Theta} + P\Theta + Gt_m = 0.$$

Ideally we would use a descriptor formulation, but currently there is no software for this case and hence we use

$$\ddot{\Theta} = -M^{-1}N\dot{\Theta} - M^{-1}P\Theta - M^{-1}Gt_m,$$

even though this introduces further errors in the data. The nominal values of the parameters are given in Table 2.

Consider now the description of the uncertainty. Based on practical considerations, we consider, in particular, the variations of the moments of inertia I_1, I_2 and I_3 of the three arms and the variations of the viscous friction coefficients C_1, C_2, C_3 and C_{p_1}, C_{p_2}. It is assumed, that the moments of inertia are constants but with possible relative error of 15% around the nominal values; similarly, the friction coefficients are with 20% relative errors.

Table 2: Nominal values of the parameters

Symbol	Value	Symbol	Value
l_1 (m)	0.5	α_1 (1/rad)	1.146
l_2 (m)	0.4	α_2 (1/rad)	1.146
h_1 (m)	0.35	α_3 (1/rad)	0.9964
h_2 (m)	0.181	C_{m_1} (Nms)	2.19×10^{-3}
h_3 (m)	0.245	C_{m_2} (Nms)	7.17×10^{-4}
m_1 (kg)	3.25	I_{m_1} (kgm^2)	2.40×10^{-5}
m_2 (kg)	1.90	I_{m_2} (kgm^2)	4.90×10^{-6}
m_3 (kg)	2.23	$C_{p_1'}$ (Nms)	0
I_1 (kgm^2)	0.654	$C_{p_2'}$ (Nms)	0
I_2 (kgm^2)	0.117	$I_{p_1'}$ (kgm^2)	7.95×10^{-3}
I_3 (kgm^2)	0.535	$I_{p_2'}$ (kgm^2)	3.97×10^{-3}
C_1 (Nms)	6.54×10^{-2}	K_1	30.72
C_2 (Nms)	2.32×10^{-2}	K_2	27.00
C_3 (Nms)	8.80×10^{-3}		

Note that in the remainder of the report, a parameter with a bar denotes its nominal value. Therefore, the actual moments of inertia are presented as

$$I_i = \bar{I}_i(1 + p_i\delta_{I_i}),\ i = 1,\ 2,\ 3,$$

where $\bar{I}_i$ is the nominal value of the corresponding moment of inertia, $p_i = 0.15$ is the maximum relative uncertainty in each of these moments and $-1 \leq \delta_{I_i} \leq 1,\ i = 1,\ 2,\ 3$. As a result the matrix M is obtained in the form

$$M = \bar{M} + M_p\Delta_I,$$

where the elements of $\bar{M}$ are determined by the nominal values of the moments of inertia,

$$\bar{M} = \begin{bmatrix} \bar{J}_1 + \bar{I}_{p_1} & \bar{l}_1\bar{M}_2 - \bar{I}_{p_1} & \bar{l}_1\bar{M}_3 \\ \bar{l}_1\bar{M}_2 - \bar{I}_{p_1} & \bar{J}_2 + \bar{I}_{p_1} + \bar{I}_{p_2} & \bar{l}_2\bar{M}_3 - \bar{I}_{p_2} \\ \bar{l}_1\bar{M}_3 & \bar{l}_2\bar{M}_3 - \bar{I}_{p_2} & \bar{J}_3 + \bar{I}_{p_2} \end{bmatrix}$$

and

$$M_p = \begin{bmatrix} \bar{I}_1 p_1 & 0 & 0 \\ 0 & \bar{I}_2 p_2 & 0 \\ 0 & 0 & \bar{I}_3 p_3 \end{bmatrix}, \Delta_I = \begin{bmatrix} \delta_{I_1} & 0 & 0 \\ 0 & \delta_{I_2} & 0 \\ 0 & 0 & \delta_{I_3} \end{bmatrix}.$$

To determine the matrix M^{-1} we use the Sherman/Morrison/Woodbury formula [5] and obtain

$$M^{-1} = \bar{M}^{-1} - \bar{M}^{-1}M_p\Delta_I(I_3 + \bar{M}^{-1}M_p\Delta_I)^{-1}\bar{M}^{-1},$$

where I_3 is the 3×3 identity matrix. The matrix M^{-1} can be represented as an upper LFT

$$M^{-1} = F_U(Q_I, \Delta_I) = Q_{I_{22}} + Q_{I_{21}}\Delta_I(I_3 - Q_{I_{11}}\Delta_I)^{-1}Q_{I_{12}},$$

where

$$Q_{I_{11}} = -\bar{M}^{-1}M_p,\ Q_{I_{12}} = \bar{M}^{-1},$$
$$Q_{I_{21}} = -\bar{M}^{-1}M_p,\ Q_{I_{22}} = \bar{M}^{-1},$$

such that

$$Q_I = \begin{bmatrix} Q_{I_{11}} & Q_{I_{12}} \\ Q_{I_{21}} & Q_{I_{22}} \end{bmatrix} = \begin{bmatrix} -\bar{M}^{-1}M_p & \bar{M}^{-1} \\ -\bar{M}^{-1}M_p & \bar{M}^{-1} \end{bmatrix}.$$

Let us now consider the uncertainties in the friction coefficients. It can be seen that C_{p_1} and C_{p_2} always appear together with C_2 and C_3 in the elements of the matrix N, and the magnitude of C_{p_1} and C_{p_2} is much smaller in comparison to that of C_2 and C_3 and, hence, the uncertainties in them have less influence in the system dynamics. We may assume

$$C_2 + C_{p_1} = (\bar{C}_2 + \bar{C}_{p_1})(1 + s_2\delta_{C_2}),$$

$$C_3 + C_{p_2} = (\bar{C}_3 + \bar{C}_{p_2})(1 + s_3\delta_{C_3}),$$

where $s_2 = 0.2,\ s_3 = 0.2$ and $-1 \le \delta_{C_2} \le 1,\ -1 \le \delta_{C_3} \le 1$. Also we set

$$C_1 = \bar{C}_1(1 + s_1\delta_{C_1}),$$

where $s_1 = 0.2$ and $-1 \le \delta_{C_1} \le 1$.

Taking into account the uncertainties in the friction coefficients we obtain

$$N = \bar{N} + \Delta N,$$

where

$$\bar{N} = \begin{bmatrix} \bar{C}_1 + \bar{C}_2 + \bar{C}_{p_1} & -\bar{C}_2 - \bar{C}_{p_1} & 0 \\ -\bar{C}_2 - \bar{C}_{p_1} & \bar{C}_2 + \bar{C}_{p_1} + \bar{C}_3 + \bar{C}_{p_2} & -\bar{C}_3 - \bar{C}_{p_2} \\ 0 & -\bar{C}_3 - \bar{C}_{p_2} & \bar{C}_3 + \bar{C}_{p_2} \end{bmatrix}$$

and

$$\Delta N = \begin{bmatrix} \bar{C}_1 s_1\delta_{C_1} + (\bar{C}_2 + \bar{C}_{p_1})s_2\delta_{C_2} & -(\bar{C}_2 + \bar{C}_{p_1})s_2\delta_{C_2} & 0 \\ -(\bar{C}_2 + \bar{C}_{p_1})s_2\delta_{C_2} & (\bar{C}_2 + \bar{C}_{p_1})s_2\delta_{C_2} & -(\bar{C}_3 + \bar{C}_{p_2})s_3\delta_{C_3} \\ & +(\bar{C}_3 + \bar{C}_{p_2})s_3\delta_{C_3} & \\ 0 & -(\bar{C}_3 + \bar{C}_{p_2})s_3\delta_{C_3} & (\bar{C}_3 + \bar{C}_{p_2})s_3\delta_{C_3} \end{bmatrix}.$$

The matrix ΔN may be represented as

$$\Delta N = N_1\Delta_C N_2,$$

where

$$N_1 = \begin{bmatrix} \bar{C}_1 s_1 & -(\bar{C}_2 + \bar{C}_{p_1})s_2 & 0 \\ 0 & (\bar{C}_2 + \bar{C}_{p_1})s_2 & -(\bar{C}_3 + \bar{C}_{p_2})s_3 \\ 0 & 0 & (\bar{C}_3 + \bar{C}_{p_2})s_3 \end{bmatrix},$$

$$N_2 = \begin{bmatrix} 1 & 0 & 0 \\ -1 & 1 & 0 \\ 0 & -1 & 1 \end{bmatrix},\ \Delta_C = \begin{bmatrix} \delta_{C_1} & 0 & 0 \\ 0 & \delta_{C_2} & 0 \\ 0 & 0 & \delta_{C_3} \end{bmatrix}.$$

The matrix $N = \bar{N} + N_1\Delta_C N_2$ may be represented as an upper LFT

$$N = F_U(Q_C, \Delta_C) = Q_{C_{22}} + Q_{C_{21}}\Delta_C(I_3 - Q_{C_{11}}\Delta_C)^{-1}Q_{C_{12}},$$

where

$$Q_{C_{11}} = 0_{3\times 3},\ Q_{C_{12}} = N_2,\ Q_{C_{21}} = N_1,\ Q_{C_{22}} = \bar{N},$$

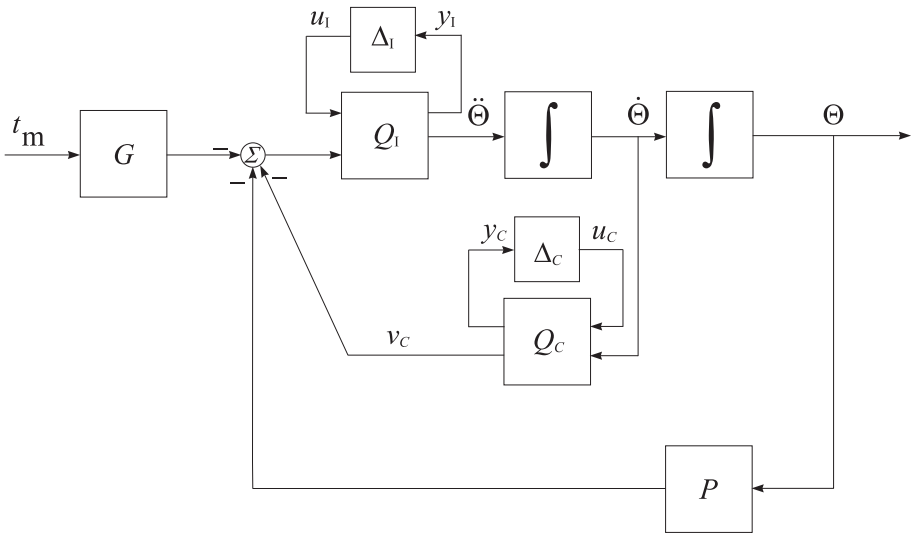

Figure 14: Block diagram of the triple inverted pendulum with uncertain parameters

such that

$$Q_C = \begin{bmatrix} Q_{C_{11}} & Q_{C_{12}} \\ Q_{C_{21}} & Q_{C_{22}} \end{bmatrix} = \begin{bmatrix} 0_{3\times 3} & N_2 \\ N_1 & \bar{N} \end{bmatrix}.$$

To represent the pendulum model as an LFT of the real uncertain parameters $\delta_{I_1},\ \delta_{I_2},\ \delta_{I_3},$ $\delta_{C_1},\ \delta_{C_2}$ and δ_{C_3}, we isolate first the uncertain parameters and denote the inputs and outputs of Δ_I and Δ_C as $y_I,\ y_C$ and $u_I,\ u_C$, respectively, as shown in Figure 14. The pendulum equations are written then as

$$\begin{array}{rcl} \begin{bmatrix} y_I \\ \ddot{\Theta} \end{bmatrix} & = & \begin{bmatrix} -\bar{M}^{-1}M_p & \bar{M}^{-1} \\ -\bar{M}^{-1}M_p & \bar{M}^{-1} \end{bmatrix} \begin{bmatrix} u_I \\ -(Gt_m + v_C + P\Theta) \end{bmatrix}, \\ \begin{bmatrix} y_c \\ v_c \end{bmatrix} & = & \begin{bmatrix} 0_{3\times 3} & N_2 \\ N_1 & \bar{N} \end{bmatrix} \begin{bmatrix} u_c \\ \dot{\Theta} \end{bmatrix}, \\ u_I & = & \Delta_I y_I, \\ u_C & = & \Delta_C y_C. \end{array}$$

The pendulum state vector

$$x = [x_1\ x_2\ x_3\ x_4\ x_5\ x_6]^T,$$

is chosen such that

$$x_1 = \Theta_1,\ x_2 = \Theta_2,\ x_3 = \Theta_3,\ x_4 = \dot{\Theta}_1,\ x_5 = \dot{\Theta}_2,\ x_6 = \dot{\Theta}_3.$$

Hence

$$\begin{bmatrix} \dot{x}_1\ \dot{x}_2\ \dot{x}_3 \end{bmatrix}^T = \dot{\Theta}$$

and

$$\begin{bmatrix} \dot{x}_4\ \dot{x}_5\ \dot{x}_6 \end{bmatrix}^T = \ddot{\Theta}.$$

As output vector we take

$$y = [\Theta_1\ \Theta_2\ \Theta_3]^T.$$

The outputs are measured by linear potentiometers, whose voltages are given by

$$y_{p_1} = \alpha_1\Theta_1,\ y_{p_2} = \alpha_2(\Theta_2 - \Theta_1),\ y_{p_3} = \alpha_3(\Theta_3 - \Theta_2).$$

Introducing the vector of the measured outputs

$$y_p = [y_{p_1}\ y_{p_2}\ y_{p_3}]^T$$

we obtain that

$$y_p = C_p\Theta,\ \ C_p = \begin{bmatrix} \alpha_1 & 0 & 0 \\ -\alpha_2 & \alpha_2 & 0 \\ 0 & -\alpha_3 & \alpha_3 \end{bmatrix}.$$

As a result we obtain the system of equations

$$\begin{array}{rcl} \begin{bmatrix} \dot{x}_1 \\ \dot{x}_2 \\ \dot{x}_3 \end{bmatrix} & = & \dot{\Theta}, \\ \begin{bmatrix} \dot{x}_4 \\ \dot{x}_5 \\ \dot{x}_6 \end{bmatrix} & = & -\bar{M}^{-1}M_p u_I - \bar{M}^{-1}(Gt_m + v_C + P\Theta), \\ y_I & = & -\bar{M}^{-1}M_p u_I - \bar{M}^{-1}(Gt_m + v_C + P\Theta), \\ y_C & = & N_2\dot{\Theta}, \\ v_C & = & N_1 u_C + \bar{N}\dot{\Theta}, \\ y & = & \Theta, \\ y_p & = & C_p\Theta, \\ u_I & = & \Delta_I y_I, \\ u_C & = & \Delta_C y_C. \end{array}$$

Excluding the variable v_C, this system of equations is represented as

$$\begin{bmatrix} \dot{x}_1 \\ \dot{x}_2 \\ \dot{x}_3 \\ \dot{x}_4 \\ \dot{x}_5 \\ \dot{x}_6 \\ -- \\ y_I \\ y_C \\ -- \\ y \\ y_p \end{bmatrix} = \left[\begin{array}{ccc|ccc|c} & & & & & & \\ 0_{3\times3} & I_{3\times3} & & 0_{3\times3} & 0_{3\times3} & & 0_{3\times2} \\ & & & & & & \\ & & & & & & \\ -\bar{M}^{-1}P & -\bar{M}^{-1}\bar{N} & & -\bar{M}^{-1}M_p & -\bar{M}^{-1}N_1 & & -\bar{M}^{-1}G \\ & & & & & & \\ ---- & ---- & - & ---- & ---- & - & ---- \\ -\bar{M}^{-1}P & -\bar{M}^{-1}\bar{N} & & -\bar{M}^{-1}M_p & -\bar{M}^{-1}N_1 & & -\bar{M}^{-1}G \\ 0_{3\times3} & N_2 & & 0_{3\times3} & 0_{3\times3} & & 0_{3\times2} \\ ---- & ---- & - & ---- & ---- & - & ---- \\ I_{3\times3} & 0_{3\times3} & & 0_{3\times3} & 0_{3\times3} & & 0_{3\times2} \\ C_p & 0_{3\times3} & & 0_{3\times3} & 0_{3\times3} & & 0_{3\times2} \end{array}\right] \begin{bmatrix} x_1 \\ x_2 \\ x_3 \\ x_4 \\ x_5 \\ x_6 \\ -- \\ u_I \\ u_C \\ -- \\ t_m \end{bmatrix}, \qquad (8)$$

$$\begin{bmatrix} u_I \\ u_C \end{bmatrix} = \begin{bmatrix} \Delta_I & 0 \\ 0 & \Delta_C \end{bmatrix} \begin{bmatrix} y_I \\ y_C \end{bmatrix}. \qquad (9)$$

In this way the pendulum model

$$\begin{bmatrix} y_I \\ y_C \\ y \\ y_p \end{bmatrix} = G_{pend} \begin{bmatrix} u_I \\ u_C \\ t_m \end{bmatrix}$$

is an eight input, twelve output system with six states, where

$$G_{pend} = \left[\begin{array}{c|cc} A & B_1 & B_2 \\ \hline C_1 & D_{11} & D_{12} \\ C_2 & D_{21} & D_{22} \end{array}\right]$$

and

$$A = \begin{bmatrix} 0_{3\times3} & I_{3\times3} \\ -\bar{M}^{-1}P & -\bar{M}^{-1}\bar{N} \end{bmatrix},\ B_1 = \begin{bmatrix} 0_{3\times3} & 0_{3\times3} \\ -\bar{M}^{-1}M_p & -\bar{M}^{-1}N_1 \end{bmatrix},\ B_2 = \begin{bmatrix} 0_{3\times2} \\ -\bar{M}^{-1}G \end{bmatrix},$$

$$C_1 = \begin{bmatrix} -\bar{M}^{-1}P & -\bar{M}^{-1}\bar{N} \\ 0_{3\times3} & N_2 \end{bmatrix},\ D_{11} = \begin{bmatrix} -\bar{M}^{-1}M_p & -\bar{M}^{-1}N_1 \\ 0_{3\times3} & 0_{3\times3} \end{bmatrix},\ D_{12} = \begin{bmatrix} -\bar{M}^{-1}G \\ 0_{3\times2} \end{bmatrix},$$

$$C_2 = \begin{bmatrix} I_{3\times3} & 0_{3\times3} \\ C_p & 0_{3\times3} \end{bmatrix},\ D_{21} = 0_{6\times6},\ D_{22} = 0_{6\times2}.$$

The uncertain behaviour of the pendulum is described by the upper LFT

$$\begin{bmatrix} y \\ y_p \end{bmatrix} = F_U(G_{pend}, \Delta_{pend})t_m$$

with diagonal uncertainty matrix

$$\Delta_{pend} = \begin{bmatrix} \Delta_I & 0 \\ 0 & \Delta_C \end{bmatrix}.$$

Consider now the actuator models. The transfer functions of the actuators are taken as first order phase-lag models

$$G_{m_1} = \frac{K_{m_1}}{T_{m_1}s+1},\ \ G_{m_2} = \frac{K_{m_2}}{T_{m_2}s+1},$$

where the nominal values of the parameters are

$$\bar{K}_{m_1} = 1.08,\ \bar{T}_{m_1} = 0.005,\ \bar{K}_{m_2} = 0.335,\ \bar{T}_{m_2} = 0.002.$$

It is assumed that the gain coefficients $K_{m_1},\ K_{m_2}$ are known with relative error 10% and the time constants $T_{m_1},\ T_{m_2}$ - with relative error 20%. The uncertain frequency responses of the actuators are shown in Figure 15. In order to account for unmodelled dynamics and nonlinear effects, the uncertainties in the actuator models are approximated by input multiplicative uncertainties which gives rise to the perturbed transfer functions

$$\tilde{G}_{m_1} = (1 + W_{m_1}\delta_{m_1})G_{m_1},\ \ \tilde{G}_{m_2} = (1 + W_{m_2}\delta_{m_2})G_{m_2},$$

where

$$|\delta_{m_1}| \le 1,\ \ |\delta_{m_2}| \le 1$$

and the uncertainty weights $W_{m_1},\ W_{m_2}$ are chosen so that

$$\frac{\left|\tilde{G}_{m_1}(j\omega) - G_{m_1}(j\omega)\right|}{|G_{m_1}(j\omega)|} < |W_{m_1}(j\omega)|,\ \ \frac{\left|\tilde{G}_{m_2}(j\omega) - G_{m_2}(j\omega)\right|}{|G_{m_2}(j\omega)|} < |W_{m_2}(j\omega)|.$$

The frequency responses of $W_{m_1},\ W_{m_2}$ are found graphically as shown in Figure 16 and then approximated by first order transfer functions. As a result one obtains

$$W_{m_1} = \frac{0.3877s + 25.6011}{1.0000s + 246.3606},\ \ W_{m_2} = \frac{0.3803s + 60.8973}{1.0000s + 599.5829}.$$

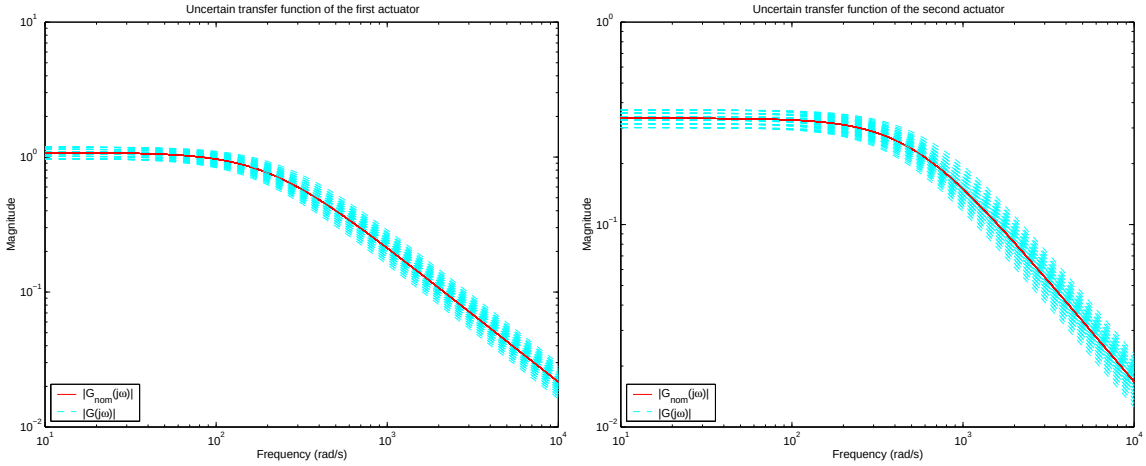

Figure 15: Uncertain frequency responses of the actuators

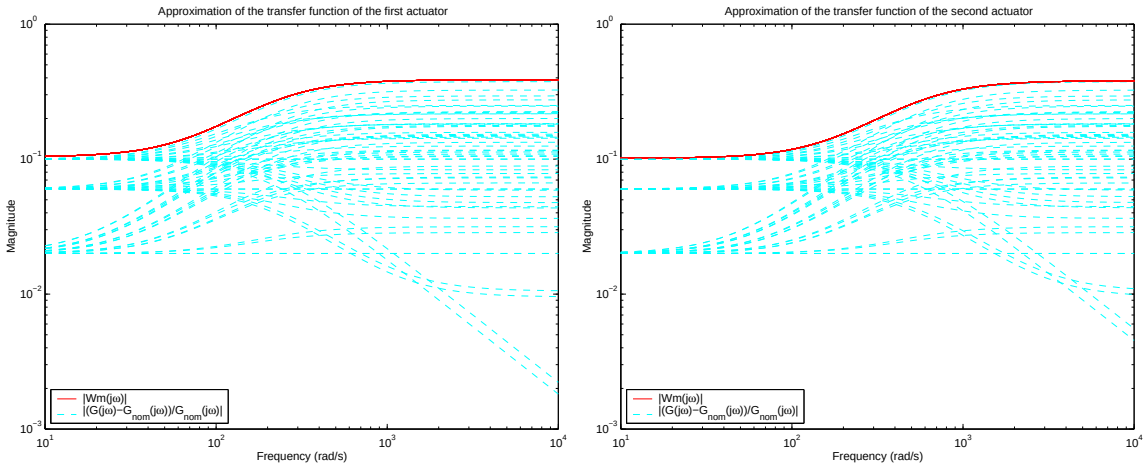

Figure 16: Actuators uncertainty approximation

Let the inputs and outputs of $\delta_{m_1},\ \delta_{m_2}$ be denoted by $y_{m_1},\ y_{m_2}$ and $u_{m_1},\ u_{m_2}$, respectively. Introducing the vectors $u = [u_1\ u_2]^T$, $u_m = [u_{m_1}\ u_{m_2}]^T$, $y_m = [y_{m_1}\ y_{m_2}]^T$, we obtain the actuators model

$$\begin{bmatrix} y_m \\ t_m \end{bmatrix} = G_m \begin{bmatrix} u_m \\ u \end{bmatrix}, \tag{10}$$

$$u_m = \Delta_m y_m, \tag{11}$$

where

$$G_m = \begin{bmatrix} 0 & 0 & W_{m_1} & 0 \\ 0 & 0 & 0 & W_{m_2} \\ G_{m_1} & 0 & G_{m_1} & 0 \\ 0 & G_{m_2} & 0 & G_{m_2} \end{bmatrix}$$

and

$$\Delta_m = \begin{bmatrix} \delta_{m_1} & 0 \\ 0 & \delta_{m_2} \end{bmatrix}.$$

The uncertain behaviour of the actuators is described by the upper LFT

$$t_m = F_U(G_m, \Delta_m)u.$$

The overall tenth order, ten inputs and fourteen outputs model of the triple inverted pendulum system consisting

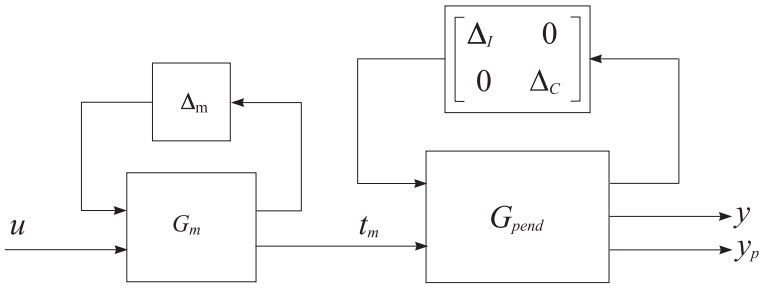

Figure 17: Triple inverted pendulum system with uncertainties

of the pendulum and the actuators is shown in Figure 17. Note that Δ_m is a complex uncertainty, while Δ_I and Δ_C are real uncertainties so that we have the case of mixed real and complex uncertainties.

Design Goals The controller synthesis problem of the triple inverted pendulum system is to find a linear, output feedback, controller $K(s)$ which has to ensure the following properties of the closed-loop system.

Nominal performance: The closed-loop system achieves nominal performance if the performance objective is satisfied for the nominal plant model

$$\begin{bmatrix} y_m \\ y_I \\ y_C \\ y \end{bmatrix} = G_{nom} \begin{bmatrix} u_m \\ u_I \\ u_C \\ u \end{bmatrix}.$$

The transfer function matrix G_{nom} is determined from the matrices G_{pend} and G_m.

The performance objective is to satisfy the inequality

$$\left\| \begin{bmatrix} W_p S \\ W_u K S \end{bmatrix} \right\|_\infty < 1, \tag{12}$$

where $S = (I + G_{nom}K)^{-1}$ is the sensitivity function of the nominal system and W_p and W_u are chosen weighting functions. This objective corresponds to the mixed S/KS sensitivity sub-optimization.

Robust stability: The closed-loop system achieves robust stability if the closed-loop system is internally stable for every possible plant dynamics $G = F_U(G_{nom}, \Delta)$, where

$$\Delta = \begin{bmatrix} \Delta_m & 0 & 0 \\ 0 & \Delta_I & 0 \\ 0 & 0 & \Delta_C \end{bmatrix}. \tag{13}$$

Robust performance: The closed-loop system must remain internally stable for every $G = F_U(G_{nom}, \Delta)$ and in addition the performance objective

$$\left\| \begin{bmatrix} W_p(I + GK)^{-1} \\ W_u K(I + GK)^{-1} \end{bmatrix} \right\|_\infty < 1 \tag{14}$$

should be satisfied for each $G = F_U(G_{nom}, \Delta)$.

In addition to those requirements it is desirable that the controller designed would have acceptable complexity, i.e., it is of reasonably low order.

According to the above considerations, the aim of the design is to determine a controller K, such that for all stable perturbations Δ with $\|\Delta\|_\infty < 1$, the perturbed closed-loop system remains stable and the perturbed weighted mixed sensitivity transfer function matrix has to satisfy the condition

$$\left\| \begin{bmatrix} W_p(I + F_U(G_{nom}, \Delta)K)^{-1} \\ W_u K(I + F_U(G_{nom}, \Delta)K)^{-1} \end{bmatrix} \right\|_\infty < 1$$

for all such perturbations.

Example 2.8 Disk Drive Servo Control System [3] (see also [11])

n	m	p
12	1	1

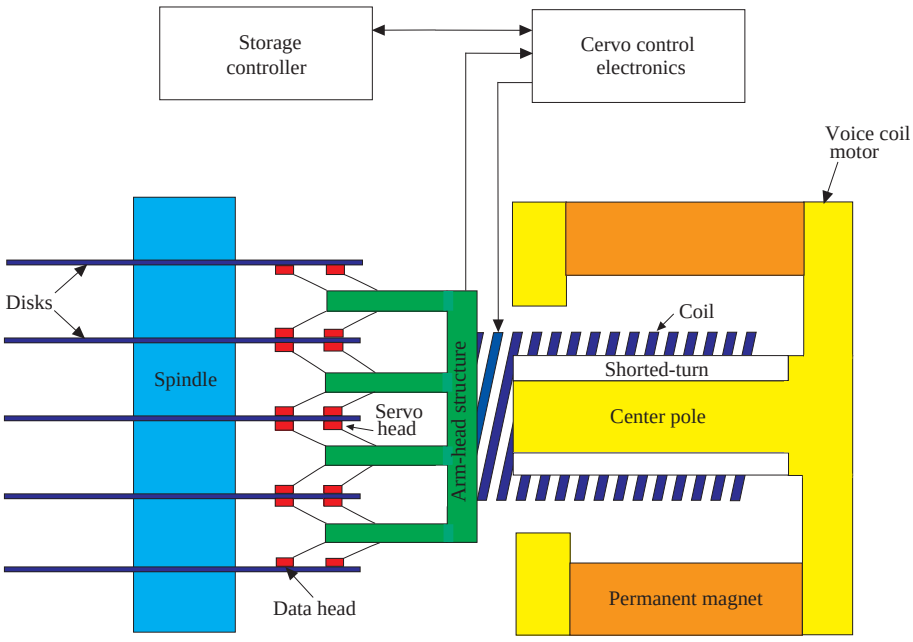

Figure 18: Schematic diagram of the Disk Drive Servo System

The schematic diagram of a Disk Drive Servo Control System is shown in Figure 18 and the block-diagram of the system is shown in Figure 19. The read/write (R/W) head is moved by a Voice Coil Motor (VCM) which is driven by the output current i_c of a power amplifier (PA). The position of the head is measured by a high

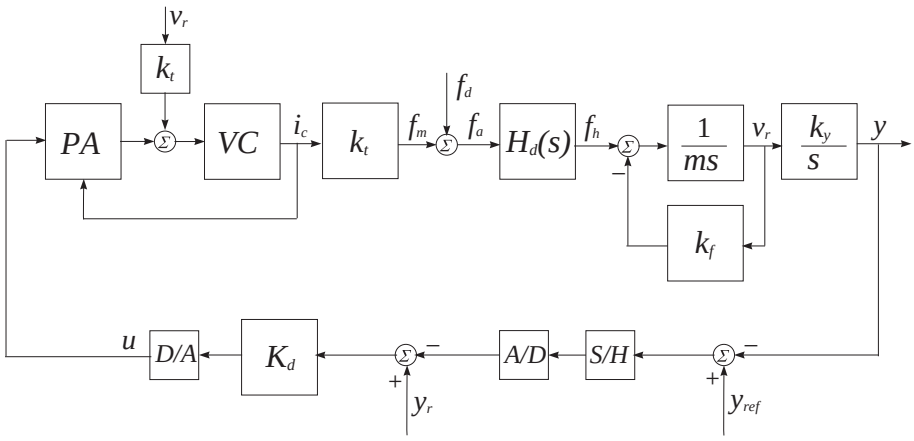

Figure 19: Block diagram of the Disk Drive Servo System

sensitive sensor. The actual position signal y is compared with the signal y_{ref} which represents the desired head position. y_r is a digital reference for the desired track. The error signal is discretized by an analog-to-digital (A/D) converter and serves as an input to the digital controller K_d which is typically implemented on a DSP chip. The output of the controller is converted to analog form by a digital-to-analog converter (D/A) and amplified by the PA. f_d denotes the force disturbance due to external shock and vibrations, power amplifier noise and digital-to-analog converter noise.

The dynamics of an ideal VCM actuator as a rigid body can be represented as a state space model in the form

$$\begin{bmatrix} \dot{y} \\ \dot{v}_r \end{bmatrix} = \begin{bmatrix} 0 & k_y \\ 0 & 0 \end{bmatrix} \begin{bmatrix} y \\ v_r \end{bmatrix} + \begin{bmatrix} 0 \\ k_v \end{bmatrix} u,$$

where u is the actuator input (in volts), y and v_r are the position (in tracks) and the velocity of the R/W head, respectively, k_y is the position measurement gain and $k_v = k_t/m$, with k_t being the current/force conversion coefficient and m being the mass of the VCM actuator. Thus the transfer function of the ideal VCM is a double integrator, i.e.

$$G_r(s) = \frac{k_v k_y}{s^2}.$$

In fact, the voice coil has a resistance R_{coil} and inductance L_{coil}, so that the voice coil admittance is

$$\frac{i_c(s)}{e_c(s)} = \frac{1/R_c}{sL_{coil}/R_c + 1},$$

where $R_c = R_{coil} + R_s$, and R_s is the current sense resistance in the power amplifier feedback. Since the corresponding electric time constant L_{coil}/R_c is large, to speedup the coil transient response an additional shortened turn, in the form of a thin layer of gold or low-oxygen content copper plated on the permanent magnet, is used. The transfer function of the voice coil with the shortened turn is

$$\frac{i_c(s)}{e_c(s)} = \frac{1}{R_c} \frac{\tau_z s + 1}{\tau_{p_1}\tau_{p_2} s^2 + (\tau_{p_1} + \tau_z)s + 1},$$

where

$$\tau_z = \frac{L_{coil} + L_{st}}{R_{st}},$$

$$\tau_{p_1} = \frac{L_{coil}}{R_c},$$
$$\tau_{p_2} = \frac{L_{st}}{R_{st}}$$

and R_{st}, L_{st} are the resistance and inductance of the shortened turn.

The parameters of the rigid body model are given in Table 3 [3].

Table 3: Rigid body model parameters and tolerances

Parameter	Description	Value	Units	Tolerance
m	moving mass of the actuator	0.200	kg	$\pm 3.0\%$
k_t	force constant	20.0	N/A	$\pm 10.0\%$
k_y	position measurement gain	10000.0	V/m	$\pm 5.0\%$
R_{coil}	coil resistance	8.00	Ω	$\pm 20.0\%$
R_s	sense resistance in the power amplifier feedback	0.25	Ω	$\pm 1.0\%$
R_{st}	shortened turn resistance	5.00	Ω	$+0, -6\%$
L_{coil}	coil inductance	0.01	H	$+0, -15\%$
L_{st}	shortened turn inductance	0.002	H	$+0, -15\%$
$e_{\max}$	saturated power amplifier voltage	34.0	V	$-0, +5\%$
k_{fric}	viscous friction coefficient	2.51	Ns/m	$\pm 7.5\%$
RPM	disk rotation rate	3623	rev/min	$\pm 3.0\%$
t_w	track width	12.5	μm	$\pm 1.0\%$

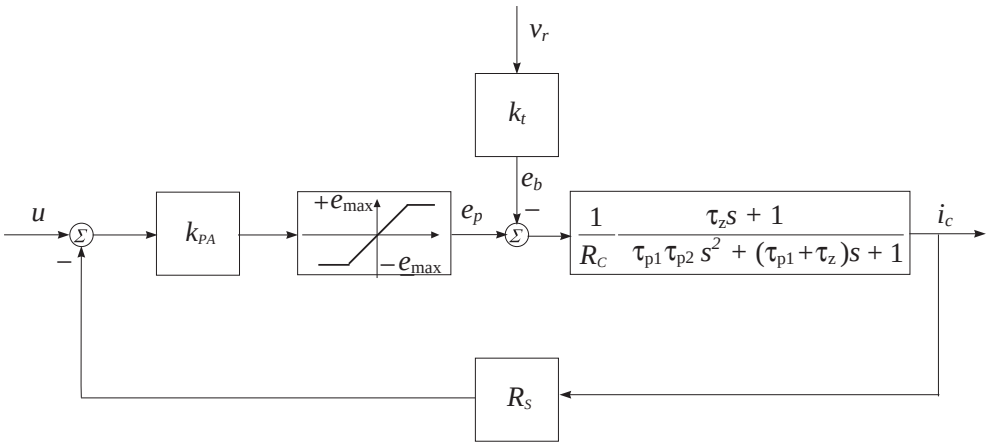

Figure 20: Block diagram of the power amplifier with voice coil

The block diagram of the power amplifier with voice coil is shown in Figure 20. The input of the voice coil is the difference $e_p - e_b$, where e_p is the output voltage of the amplifier and $e_b = k_t v_r$ is the back emf which is generated during the moving of the coil in the magnetic field. Since the saturation voltage of the amplifier is $e_{\max}$, the maximum steady state current in the coil is $e_{\max}/R_c$. There is a negative current feedback in the amplifier which is realized by the resistance R_s. In the study of the linearized system the back emf and the amplifier saturation are neglected and as a result we obtain the transfer function

$$G_{vca} = \frac{i_c(s)}{u(s)} = \frac{k_{PA}(\tau_z s + 1)}{R_c\tau_{p1}\tau_{p2}s^2 + [R_c\tau_{p1} + (R_c + k_{PA}R_s)\tau_z]s + R_c + K_{PA}R_s}.$$

In the given case the amplifier gain k_{PA} is chosen equal to 11, so that the loop gain

$$\frac{k_{PA}}{R_c + K_{PA}R_s}$$

is equal to 1. This means that in the absence of back emf the amplifier will saturate for an input voltage u greater than $e_{\max}/R_c$ (about 4.12 V).

In practice we must also take into account the viscous friction force $k_f v_r$ and the high frequency resonance modes of the head disk assembly represented by the transfer function $H_d(s)$. $H_d(s)$ consists of four flexible (resonance) modes and is obtained as

$$H_d(s) = \sum_{j=1}^{4} \frac{b_{2j}\omega_j s + b_{2j-1}\omega_j^2}{s^2 + 2\xi_j\omega_j s + \omega_j^2}$$

(see Figure 21).

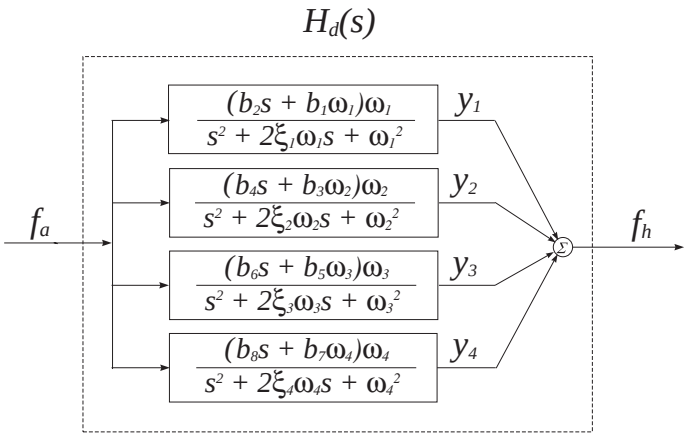

Figure 21: Flexible mode transfer functions

Here ω_j, ξ_j and b_{2j}, b_{2j-1} are the resonance frequency, the damping coefficient and the coupling coefficients for the j-th mode, for j=1,...,4. The resonance parameters are determined experimentally and are shown in Table 4 [3].

As is seen from Table 3 and Table 4, the number of uncertain parameters is greater than 25, which complicates very much the analysis and design of the disk drive servo system. In this study we shall concentrate on those uncertainty parameters which influence most the closed loop system behaviour. For convenience, the open loop

Table 4: Dynamic (resonance) parameters and tolerances

Parameter	Description	Value	Units	Tolerance
ω_1	resonance: VCM isolator	$2\pi 70$	rad/s	$\pm 5.0\%$
ω_2	resonance: head suspension	$2\pi 2200$	rad/s	$\pm 10.0\%$
ω_3	resonance: actuator arm carrier	$2\pi 4000$	rad/s	$\pm 5.0\%$
ω_4	resonance: coil structure	$2\pi 9000$	rad/s	$\pm 5.0\%$
b_1	first resonance coupling	-0.00575	-	$\pm 7.0\%$
b_2	first resonance coupling	-0.0000115	1/s	$\pm 7.0\%$
b_3	second resonance coupling	0.0230	-	$\pm 10.0\%$
b_4	second resonance coupling	0.0	1/s	$\pm 7.0\%$
b_5	third resonance coupling	0.8185	-	$\pm 5.0\%$
b_6	third resonance coupling	0.0	1/s	$\pm 10.0\%$
b_7	fourth resonance coupling	0.1642	-	$\pm 5.0\%$
b_8	fourth resonance coupling	0.0273	1/s	$\pm 10.0\%$
ξ_1	first resonance damping	0.05	-	$\pm 10.0\%$
ξ_2	second resonance damping	0.005	-	$\pm 40.0\%$
ξ_3	third resonance damping	0.05	-	$\pm 40.0\%$
ξ_4	fourth resonance damping	0.005	-	$\pm 50.0\%$

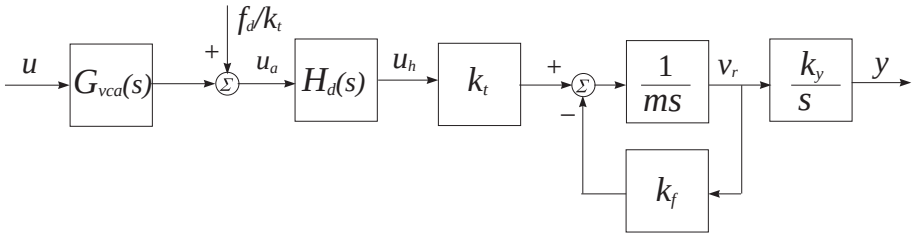

Figure 22: Transformed block diagram of the open-loop contour

system blocks are rearranged as shown in Figure 22.

Consider first the derivation of the uncertainty model for the resonance modes. For each of the four modes we have the similar transfer function so we shall describe here only the first mode. Its state space model is (for the simplicity of notations we drop some subscripts)

$$\begin{aligned} \dot{x}_1 &= \omega x_2, \\ \dot{x}_2 &= \omega(-x_1 - 2\xi x_2 + u), \\ y_1 &= b_1 x_1 + b_2 x_2. \end{aligned}$$

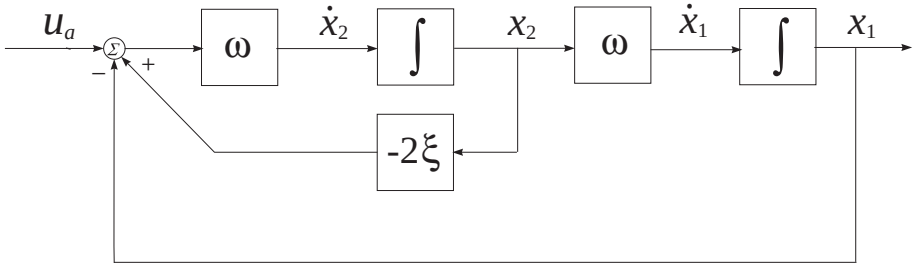

Figure 23: Block diagram of a flexible mode

The block diagram of the state equations of a flexible mode is shown in Figure 23. The variations in the frequency ω and the damping coefficient ξ are represented as

$$\omega = \bar{\omega}(1 + p_\omega \delta_\omega)$$

and

$$\xi = \bar{\xi}(1 + p_\xi \delta_\xi),$$

respectively, where $\bar{\omega}$ and $\bar{\xi}$ are the nominal values, p_ω and p_ξ are the maximum relative uncertainties and

$$-1 \leq \delta_\omega \leq 1,$$

$$-1 \leq \delta_\xi \leq 1$$

are the relative variations in these parameters.

The parameter ω may be represented as an upper Linear Fractional Transformation (LFT) in δ_ω

$$\omega = F_U(M_\omega, \delta_\omega)$$

with

$$M_\omega = \begin{bmatrix} 0 & \bar{\omega} \\ p_\omega & \bar{\omega} \end{bmatrix}$$

and the parameter ξ may be represented as an upper LFT in δ_ξ,

$$\xi = F_U(M_\xi, \delta_\xi)$$

with

$$M_\xi = \begin{bmatrix} 0 & \bar{\xi} \\ p_\xi & \bar{\xi} \end{bmatrix}$$

(see [1, 17]). The block diagram of a flexible mode with uncertain parameters is given in Figure 24. From this diagram we derive the following equations

$$\begin{bmatrix} y_\omega \\ \dot{x}_2 \end{bmatrix} = \begin{bmatrix} 0 & \bar{\omega} \\ p_\omega & \bar{\omega} \end{bmatrix} \begin{bmatrix} u_\omega \\ u - 2v_\xi - x_1 \end{bmatrix},$$

$$\begin{bmatrix} z_\omega \\ \dot{x}_1 \end{bmatrix} = \begin{bmatrix} 0 & \bar{\omega} \\ p_\omega & \bar{\omega} \end{bmatrix} \begin{bmatrix} v_\omega \\ x_2 \end{bmatrix},$$

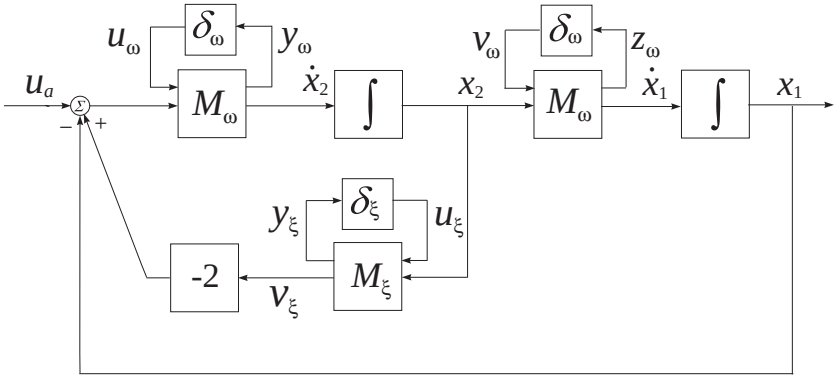

Figure 24: Flexible Mode with uncertain parameters

$$\begin{bmatrix} y_\xi \\ v_\xi \end{bmatrix} = \begin{bmatrix} 0 & \bar{\xi} \\ p_\omega & \bar{\xi} \end{bmatrix} \begin{bmatrix} u_\xi \\ x_2 \end{bmatrix},$$

and

$$y = \begin{bmatrix} b_1 & b_2 \end{bmatrix} \begin{bmatrix} x_1 \\ x_2 \end{bmatrix}.$$

From these equations we obtain the perturbed model of a flexible mode in the form of

$$\left[\begin{array}{c} \dot{x}_1 \\ \dot{x}_2 \\ -- \\ y_\omega \\ z_\omega \\ y_\xi \\ -- \\ y \end{array}\right] = \left[\begin{array}{cc|ccc|c} 0 & \bar{\omega} & 0 & p_\omega & 0 & 0 \\ -\bar{\omega} & -2\bar{\omega}\xi & p_\omega & 0 & -2\bar{\omega}p_\xi & \bar{\omega} \\ -- & -- & -- & -- & -- & -- \\ -\bar{\omega} & -2\bar{\omega}\xi & p_\omega & 0 & -2\bar{\omega}p_\xi & \bar{\omega} \\ 0 & \bar{\omega} & 0 & 0 & 0 & 0 \\ 0 & \bar{\xi} & 0 & 0 & 0 & 0 \\ -- & -- & -- & -- & -- & -- \\ b_1 & b_2 & 0 & 0 & 0 & 0 \end{array}\right] \left[\begin{array}{c} x_1 \\ x_2 \\ -- \\ u_\omega \\ v_\omega \\ u_\xi \\ -- \\ u_a \end{array}\right].$$

A generalized block diagram of a flexible mode with four inputs and four outputs is shown in Figure 25. Consider

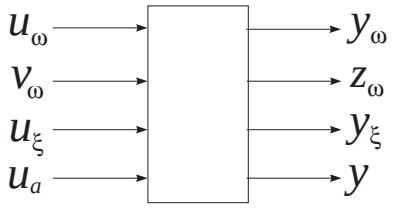

Figure 25: Generalized block diagram of a flexible mode

now the derivation of the uncertain model of the rigid body part of the system taking into account the viscous friction. The block diagram of this part of the system is shown in Figure 26. The state space equations in this

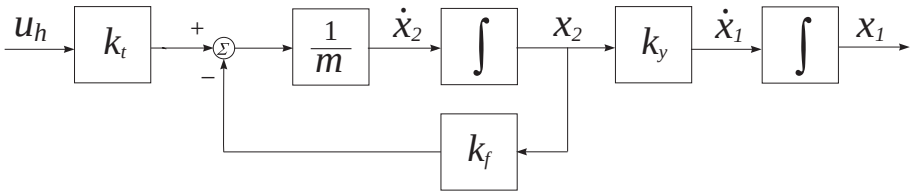

Figure 26: Block diagram of the rigid body model

case are

$$\begin{aligned} \dot{x}_1 &= k_y x_2, \\ \dot{x}_2 &= -\tfrac{k_f}{m} x_2 + \tfrac{k_t}{m}(y_1 + y_2 + y_3 + y_4). \end{aligned}$$

The uncertain parameters of the rigid body model are taken as

$$\begin{aligned} k_t &= \bar{k}_t(1 + p_{k_t}\delta_{k_t}), \\ k_y &= \bar{k}_y(1 + p_{k_y}\delta_{k_y}), \\ k_f &= \bar{k}_f(1 + p_{k_f}\delta_{k_f}) \end{aligned}$$

with

$$-1 \le \delta_{k_t} \le 1,$$

$$-1 \le \delta_{k_y} \le 1,$$

$$-1 \le \delta_{k_f} \le 1.$$

These parameters are represented as LFT in the relative uncertainties $\delta_{k_t},\ \delta_{k_y},\ \delta_{k_f}$:

$$\begin{aligned} k_t &= F_U(M_{k_t}, \delta_{k_t}), \\ k_y &= F_U(M_{k_y}, \delta_{k_y}), \\ k_f &= F_U(M_{k_f}, \delta_{k_f}), \end{aligned}$$

where

$$M_{k_t} = \begin{bmatrix} 0 & \bar{k}_t \\ p_{k_t} & \bar{k}_t \end{bmatrix}, \quad M_{k_y} = \begin{bmatrix} 0 & \bar{k}_y \\ p_{k_y} & \bar{k}_y \end{bmatrix}, \quad M_{k_f} = \begin{bmatrix} 0 & \bar{k}_f \\ p_{k_f} & \bar{k}_f \end{bmatrix}.$$

As a result we obtain the block diagram shown in Figure 27.

From this block diagram in a way similar to the case of a flexible mode we derive the following rigid body uncertainty model

$$\begin{bmatrix} \dot{x}_1 \\ \dot{x}_2 \\ -- \\ y_{k_t} \\ y_{k_y} \\ y_{k_f} \\ -- \\ y \end{bmatrix} = \left[\begin{array}{cc|ccc|c|cc} 0 & \bar{k}_y & 0 & p_{k_y} & 0 & 0 \\ 0 & -\frac{\bar{k}_f}{m} & \frac{p_{k_t}}{m} & 0 & -\frac{p_{k_f}}{m} & \frac{\bar{k}_t}{m} \\ \hline 0 & 0 & 0 & 0 & 0 & \bar{k}_t \\ 0 & \bar{k}_y & 0 & 0 & 0 & 0 \\ 0 & \bar{k}_f & 0 & 0 & 0 & 0 \\ \hline 1 & 0 & 0 & 0 & 0 & 0 \end{array}\right] \begin{bmatrix} x_1 \\ x_2 \\ -- \\ u_{k_t} \\ u_{k_y} \\ u_{k_f} \\ -- \\ u_h \end{bmatrix}.$$

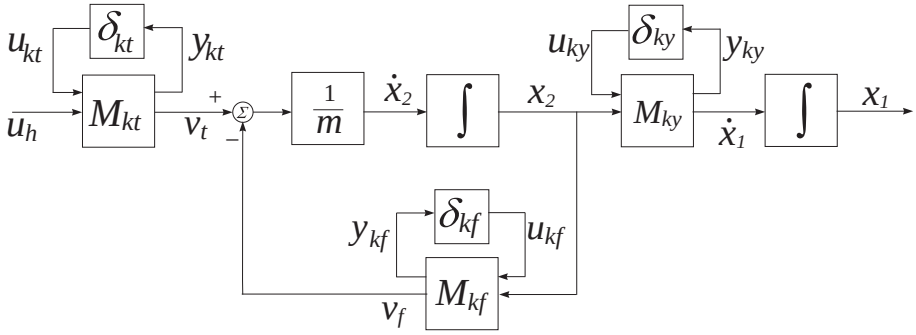

Figure 27: Rigid Body model with uncertain parameters

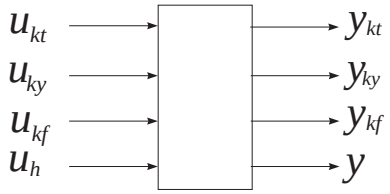

Figure 28: Generalized block diagram of the Rigid Body model with uncertain parameters

The generalized block diagram of the rigid body model with four inputs and four outputs is shown in Figure 28.

We may connect the uncertain models of the four resonance modes with the uncertain model of the rigid body, as shown in Figure 29. Overall, we have eleven uncertain parameters but four of them (ω_1, ω_2, ω_3 and ω_4) are repeated twice. By 'pulling out' the uncertain parameters from the nominal part of the model, we obtain a perturbed plant model in the form of an upper LFT as shown in Figure 30 with a 15×15 matrix Δ,

$$\Delta = \text{diag}(\delta_{\omega_1}, \delta_{\omega_1}, \delta_{\xi_1}, \delta_{\omega_2}, \delta_{\omega_2}, \delta_{\xi_2}, \delta_{\omega_3}, \delta_{\omega_3}, \delta_{\xi_3}, \delta_{\omega_4}, \delta_{\omega_4}, \delta_{\xi_4}, \delta_{k_t}, \delta_{k_y}, \delta_{k_f}),$$

which contains the uncertain parameters. The system model is of order twelve. In Figures 31 and 32 we show the Bode plot of the parallel connection $H_d(s)$ of the flexible modes with uncertain parameters varying between the lower and upper bounds.

The block diagram of the closed-loop system, which includes the feedback structure and the controller as well as the elements reflecting the model uncertainty and the performance objectives, is shown in Figure 33. The system has a reference input (r), an input disturbance (d) and two output costs (e_y and e_u). The system M is an ideal model to match the closed loop system to. The rectangle, shown by a dashed line, represents the plant transfer function matrix G. Inside the rectangle is the nominal model G_{nom} of the disk drive control system and the block Δ, which parameterizes the model uncertainties. The matrix Δ is unknown, but it has a diagonal structure and norm bound $\|\Delta\|_\infty < 1$. The performance objective requires the transfer matrices from r and d to e_y and e_u to be small in the sense of $\|.\|_\infty$, for all possible uncertain matrices Δ. The transfer matrices W_p and W_u are used to reflect the relative significance of the different frequency ranges for which the performance is required. Hence, the performance objective can be recast, with possible slight conservativeness, as that the $\|.\|_\infty$ of the transfer

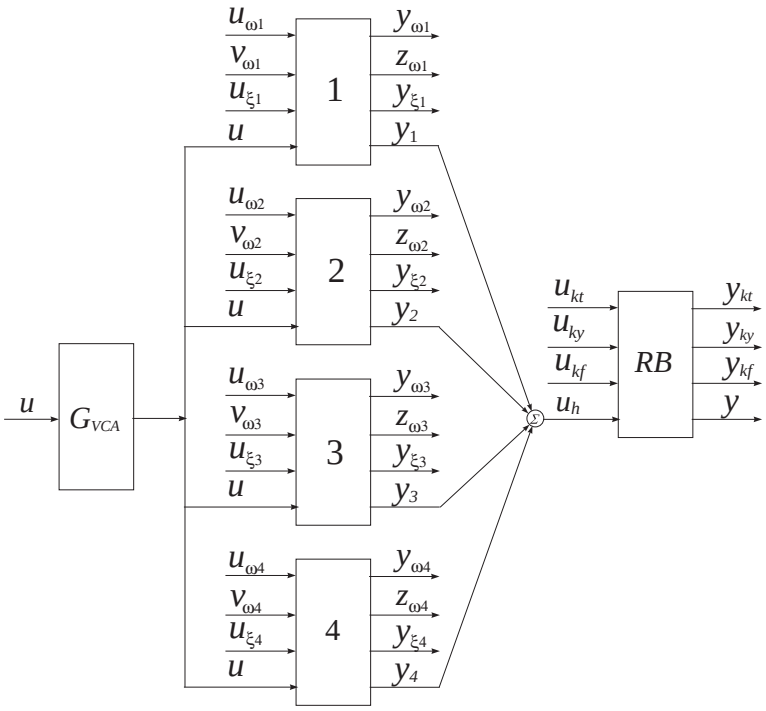

Figure 29: Plant model with uncertainties

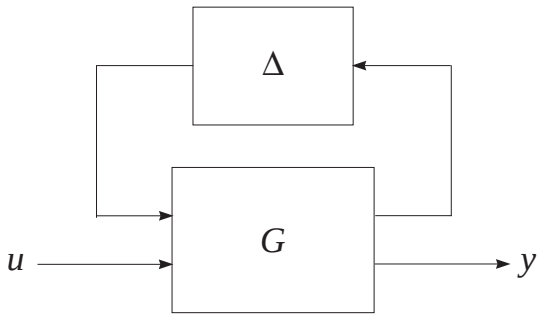

Figure 30: Plant model in the form of an upper LFT

function matrix from r and d to e_y and e_u is less than 1.

It is possible to show that

$$\begin{bmatrix} e_y \\ e_u \end{bmatrix} = \begin{bmatrix} W_p(S_oGK - M) & W_pS_oG \\ W_uS_iK & -W_uKS_oG \end{bmatrix} \begin{bmatrix} r \\ d \end{bmatrix},$$

where $S_i = (I + KG)^{-1}$, $S_o = (I + GK)^{-1}$ are the input and output sensitivities, respectively. Note that S_oG is the transfer function between d and y. Based on Figure 33, the total interconnection block diagram of the closed-loop system is shown in Figure 34. The transfer function matrix P is determined by the matrices G_{nom}, W_p and W_u. w and z denote the inputs to and outputs from the uncertainty block Δ, respectively.

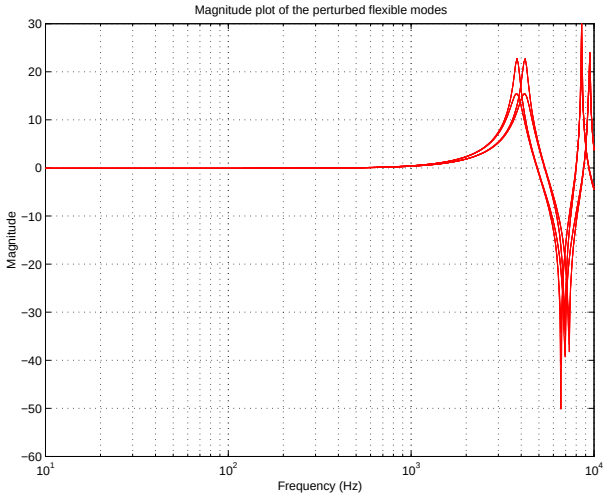

Figure 31: Magnitude plot of the perturbed flexible modes

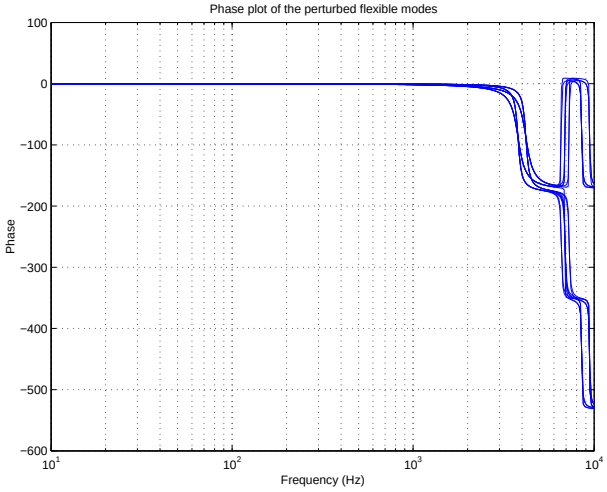

Figure 32: Phase plot of the perturbed flexible modes

Some realistic requirements of the closed-loop system dynamics, which have been considered in the design of the Disk Drive Servo using classical frequency response methods, are as follows.

Peak closed-loop gain	$<$	4 dB
Open-loop gain	$>$	20 dB at 100 Hz
Steady state error	$<$	0.375 μm
Bandwidth	$>$	800 Hz
Attenuation at 60 Hz		30 dB
Attenuation at 1.6 kHz		10 dB
Attenuation at 4 kHz		22 dB
Gain Margin	$>$	10 dB
Phase margin	$>$	45 deg

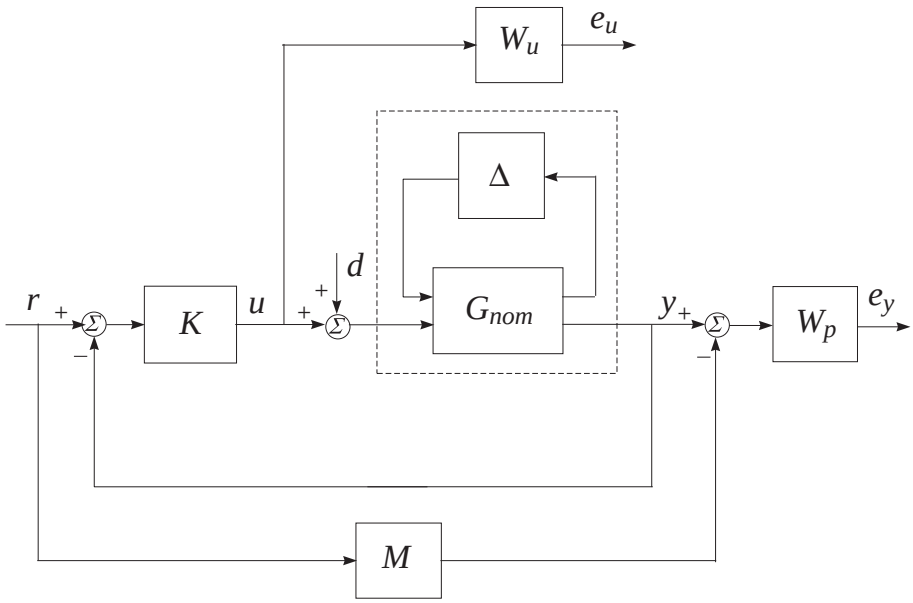

Figure 33: Closed-loop system with performance specifications

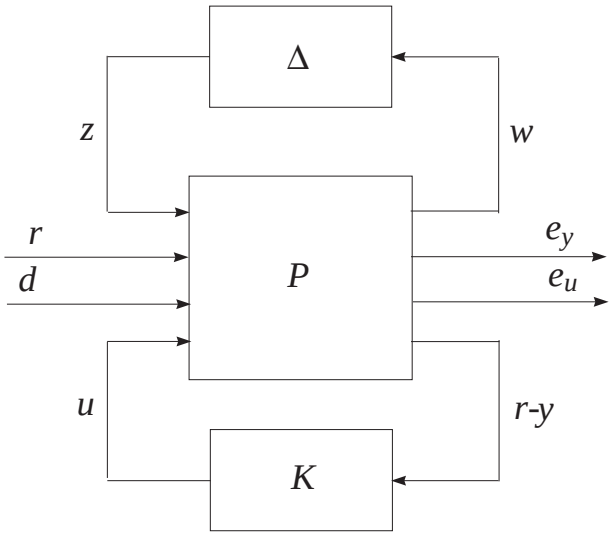

Figure 34: Total interconnection structure of the closed-loop system

In addition, it is necessary to have small control action in order to avoid the power amplifier saturation. **Design Goals**

The controller synthesis problem of the Disk Drive Servo System is to find a linear, output feedback, controller $K(s)$ which has to ensure the following properties of the closed-loop system.

Nominal performance: The closed-loop system achieves nominal performance if the performance objective is satisfied for the nominal plant model.

The performance objective is to satisfy the inequality

$$\left\| \begin{bmatrix} W_p(S_oG_{nom}K - M) & W_pS_oG_{nom} \\ W_uS_iK & -W_uKS_oG_{nom} \end{bmatrix} \right\|_\infty < 1. \tag{15}$$

This objective is similar to the usual mixed S/KS sensitivity optimization and it enables robustness and performance criteria to be met incorporating performance specifications in the matching model M. The four functions to be minimized are described in Table 5. The interconnection structure, corresponding to the nominal per-

Table 5: $\mathcal{H}_\infty$ functions to be minimized

Function	Description
$W_p(S_oGK - M)$	Weighted difference between the ideal and actual closed systems
W_pS_oG	Weighted disturbance sensitivity
W_uS_iK	Weighted control effort due to reference input
W_uKS_oG	Weighted control effort due to the disturbance

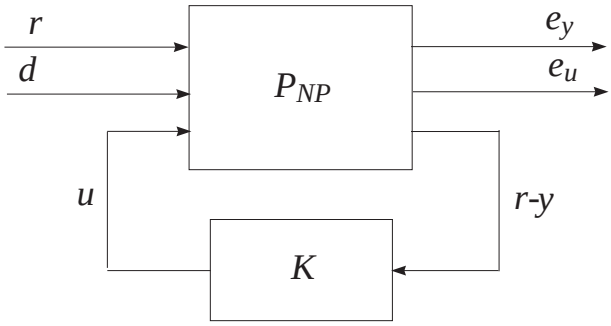

Figure 35: Interconnection structure, corresponding to nominal performance

formance analysis, is shown in Figure 35. The transfer function matrix P_{NP} is determined from the matrix P, shown in Figure 34, neglecting the inputs to and the outputs from the uncertainty block Δ.

Robust stability: The closed-loop system achieves robust stability if the closed-loop system is internally stable for each possible plant dynamics $G = F_U(G_{nom}, \Delta)$. The interconnection structure, corresponding to the robust stability analysis, is shown in Figure 36. The transfer function matrix P_{RS} is determined from the matrix P, shown in Figure 34, neglecting the inputs r, d and the outputs e_y, e_u.

Robust performance: The closed-loop system must remain internally stable for each $G = F_U(G_{nom}, \Delta)$ and in addition the performance objective

$$\left\| \begin{bmatrix} W_p(S_oGK - M) & W_pS_oG \\ W_uS_iK & -W_uKS_oG \end{bmatrix} \right\|_\infty < 1 \tag{16}$$

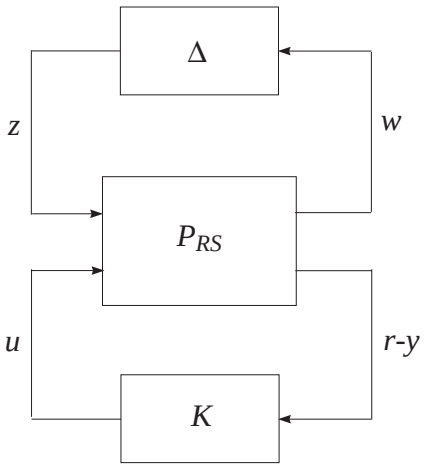

Figure 36: Interconnection structure, corresponding to robust stability

should be satisfied for each $G = F_U(G_{nom}, \Delta)$. This means that the structured singular value, corresponding to the transfer function matrix from (Figure 34) $\begin{bmatrix} z \\ r \\ d \end{bmatrix}$ to $\begin{bmatrix} w \\ e_y \\ e_u \end{bmatrix}$ should be less than 1, with regard to $\begin{bmatrix} \Delta & 0 \\ 0 & \Delta_F \end{bmatrix}$, where Δ_F is a fictitious 2×2 complex uncertainty block. In addition to these requirements it is desirable that the designed controller has acceptable complexity, i.e. it is of reasonably low order.

According to the above considerations, the aim of the design is to determine a controller K, such that for all stable perturbations Δ with $\|\Delta\|_\infty < 1$, the perturbed closed-loop system remains stable and the performance objective is satisfied for all such perturbations.

References

[1] G. J. Balas, J. C. Doyle, K. Glover, A. Packard, and R. Smith. μ-analysis and synthesis toolbox users guide. The Mathworks Inc., Natick, MA, 1998.

[2] P. Benner, R. Byers, V. Mehrmann, and H. Xu. Robust numerical methods for robust control. In preparation.

[3] G.F. Franklin, J.D. Powell and M.L. Workman. *Digital Control of Dynamic Systems*, 3rd ed. Addison-Wesley Pub. Co., 1998.

[4] K. Furuta, T. Ochia, and N. Ono. Attitude control of a triple inverted pendulum. Int. J. Control, vol. 39, 1984, pp. 1351-1365.

[5] G.H. Golub and C.F. Van Loan. *Matrix Computations*. Johns Hopkins University Press, Baltimore, third edition, 1996.

[6] D.-W. Gu, P. Hr. Petkov, and M.M. Konstantinov. Direct formulae for the H_∞ sub-optimal central controller. NICONET Report 1998–7, The Working Group on Software (WGS), 1998. Available from `http://www.win.tue.nl/niconet/NIC2/reports.html`.

[7] D.W. Gu,, P.Hr. Petkov, and M. Konstantinov. An introduction to H_∞ optimisation designs. NICONET Report 1999-4, May 1999. Available from `ftp://wgs.esat.kuleuven.ac.be/pub/WGS/REPORTS`.

[8] J.M. Maciejowski *Multivariable Feedback Design*. Addison-Wesley, Wokingham, U.K., 1989.

[9] The MathWorks, Inc., Cochituate Place, 24 Prime Park Way, Natick, Mass, 01760. *The MATLAB Robust Control Toolbox, Version 2.0b*, 1994.

[10] P.Hr. Petkov, D.W. Gu, and M. Konstantinov. Robust control of a triple inverted pendulum using μ-synthesis. NICONET Report 2001-1, Jan. 2001. Available from `http://www.win.tue.nl/wgs/niconet.html`.

[11] P.Hr. Petkov, D.-W. Gu, and M.M. Konstantinov. Robust Control of a Disk Drive Servo System. NICONET Report 2001-07, June 2001. Available from `http://www.win.tue.nl/wgs/niconet.html`.

[12] P. Hr. Petkov, D.-W. Gu, and M.M. Konstantinov. Fortran 77 routines for H_∞ and H_2 design of continuous-time linear control systems controller. NICONET Report 1998–8, The Working Group on Software (WGS), 1998. Available from `http://www.win.tue.nl/niconet/NIC2/reports.html`.

[13] Skogestad, S. and I. Postlethwaite (1996). *Multivariable Feedback Control*. John Wiley & Sons, Chichester, U.K.

[14] J. F. Whidborne, G. Murad, D.-W. Gu, and I. Postlethwaite. Int. J. Control, vol. 61, 1995, pp. 589–640.

[15] B. Wie and D. Bernstein. Benchmark problems for robust control design. Proc. American Control Conference, Chicago, IL, June 1992, pp. 2047–2048.

[16] B. Wie and D. Bernstein. Benchmark problems for robust control design. Journal of Guidance, Control and Dynamics, Vol. 15, 1992, pp. 1057–1059.

[17] K. Zhou, J.C. Doyle, and K. Glover. *Robust and Optimal Control*. Prentice Hall, Upper Saddle River, New Jersey, 1996.

Appendix. M-files of uncertainty models

Example 1.1

File: **mod_11**

```
% Example 1.1
A = [ 0    0     1.1320      0       -1
      0 -0.0538 -0.1712      0     0.0705
      0    0        0        1        0
      0  0.0485     0    -0.8556  -1.0130
      0 -0.2909     0     1.0532  -0.6859];
%
B = [  0       0      0
     -0.1200   1      0
      0        0      0
      4.4190   0   -1.6650
      1.5750   0   -0.0732 ];
%
C = [1  0  0  0  0
     0  1  0  0  0
     0  0  1  0  0];
%
d = zeros(3,3);
%
G = pck(A,B,C,D);
```

Example 2.1

File: **mod_21**

```
% Example 2.1
%
% Default values
alpha = 1;
beta = 1;
delta = 1;
eta = 1;
e1 = 0;
e2 = 0;
%
A = [-1  0
      0 -1];
%
B = [e1  0   1
     0   e2  1];
%
C = [alpha  0
       0    beta
     delta  eta];
%
D = [0.5   0    0
     0     0.5  1
     0     1    0];
%
G = pck(A,B,C,D);
```

Example 2.2

File: **mod_22**

```
% Example 2.2
%
% Default value
alpha = 10^(-10);
%
A = [-alpha   0   1  -2          1
        0   -100  0   0          0
        0     0   0  -2*alpha  alpha
        0     0   0   0          1
        0     0   0   3          2];
%
B = [1      0
     0     -90
     alpha  0
     0      0
     0      0];
%
C = [1  0  0  0  0
     0  1  0  0  0
     0  0  1 -2  1];
%
D = [ 0  0
      0  1
      1  0];
%
G = pck(A,B,C,D);
```

Example 2.3

File: **mod_23**

```
% Example 2.3
%
% Default value
alpha = 3;
%
A = [2  -1
     0  -1];
%
B = [ 0  1  -1
      0  1  -2];
%
C = [1  0
     0  1
     4 -2];

%
D = [alpha  0   0
        0  -1   1
        0   1   0];
%
G = pck(A,B,C,D);
```

Example 2.4 (Mass/damper/spring system)

File: **mod_mds**

```
% Uncertainty model of the Mass/Damper/Spring system
%
% parameter values
m = 3;
c = 1;
k = 2;
pm = 0.4;
pc = 0.2;
pk = 0.3;
%
A = [  0     1
     -k/m  -c/m];
B1 = [  0    0        0
      -pm  -pc/m   -pk/m];
B2 = [ 0
      1/m];
C1 = [-k/m  -c/m
       0     c
       k     0 ];
C2 = [ 1 0 ];
D11 = [ -pm  -pc/m  -pk/m
         0     0      0
         0     0      0 ];
D12  = [1/m
        0
        0  ];
D21 = [0 0 0];
D22 = 0;
G = pck(A,[B1,B2],[C1;C2],[D11 D12;D21 D22]);
```

Example 2.5 (Two-mass-spring system)

File: **mod_spr**

```
% Uncertainty model of two-mass-spring example problem
%
% parameter values
k = 1.25;
m1 = 1;
m2 = 1;
pk = 0.24;
pm1 = 0.1;
pm2 = 0.1;
%
A = [  0     0   1   0
       0     0   0   1
     -k/m1  k/m1 0   0
      k/m2 -k/m2 0   0 ];
B1 = [  0       0     0
        0       0     0
      -pk/m1  -pm1    0
       pk/m2    0   -pm2];
B2 = [0    0    0
      0    0    0
     1/m1  0   1/m1
      0   1/m2  0 ];
C1 = [  k    -k   0   0
      -k/m1  k/m1 0   0
       k/m2 -k/m2 0   0 ];
C2 = [0 1 0 0];
D11 = [   0     0    0
       -pk/m1 -pm1   0
        pk/m2   0  -pm2];
D12  = [ 0    0    0
        1/m1  0   1/m1
         0   1/m2  0  ];
D21 = [0 0 0];
D22 = [0 0 0];
G = pck(A,[B1,B2],[C1;C2],[D11 D12;D21 D22]);
```

Example 2.6 (IFAC93 benchmark example)

File: **mod_ifac**

```
% IFAC93 benchmark example problem
%
% parameter values
T1 = 5;
T2 = 0.4;
w0 = 5;
z = 0.3;
K = 1;
%
% Stress level 2
p_K  = 0.15;
p_T1 = 0.06;
p_T2 = 0.25;
p_w0 = 0.5;
p_z  = 0.5;
%
mat_K = [ 0    K
         p_K   K];
%
mat_w01 = [ 0   w0
           p_w0 w0];
%
mat_w02 = [ 0   w0
           p_w0 w0];
%
mat_z = [ 0   z
         p_z  z];
%
mat_T1 = [-p_T1   1/T1
          -p_T1   1/T1];
%
mat_T2 = [  0      T2
           p_T2    T2];
%
int1 = nd2sys([0 1],[1 0]);
int2 = nd2sys([0 1],[1 0]);
int3 = nd2sys([0 1],[1 0]);
```

```
%
systemnames = ' mat_K mat_w01 mat_w02 mat_z mat_T1 mat_T2 int1 int2 int3 ';
inputvar = '[ pert{6}; control ]';
temp =  '[ mat_K(1); mat_w01(1); mat_w02(1); mat_z(1); mat_T1(1); mat_T2(1);';
outputvar = [ temp ' mat_T1(2) ]'];
input_to_mat_K = '[ pert(1); control ]';
input_to_mat_w01 = '[ pert(2); mat_K(2)-2.*mat_z(2)-int2]';
input_to_mat_w02 = '[ pert(3); int1 ]';
input_to_mat_z = '[ pert(4); int1 ]';
input_to_mat_T1 = '[ pert(5); int3 - mat_T2(2) ]';
input_to_mat_T2 = '[ pert(6); int2 ]';
input_to_int1 = '[ mat_w01(2) ]';
input_to_int2 = '[ mat_w02(2) ]';
input_to_int3 = '[ int2 - mat_T1(2) ]';
sysoutname = 'G';
cleanupsysic = 'yes';
sysic
```

Example 2.7 (Triple inverted pendulum system)

File: **mod_pend**

```
% Uncertainty model of triple inverted pendulum
%
% parameter values
l1 = 0.5; l2 = 0.4; h1 = 0.35; h2 = 0.181; h3 = 0.245;
m1 = 3.25; m2 = 1.9; m3 = 2.23;
i1 = 0.654; i2 = 0.117; i3 = 0.535;
c1 = 0.0654; c2 = 0.0232; c3 = 0.0088;
alf1 = 1.146; alf2 = 1.146; alf3 = 0.9964;
cd1 = 0.00219; cd2 = 0.000717;
id1 = 0.000024; id2 = 0.0000049;
cp1p = 0.; cp2p = 0.;
ip1p = 0.00795; ip2p = 0.00397;
k1 = 30.72; k2 = 27.0;
g = 9.81;
mm1 = m1*h1 + m2*l1 + m3*l1;
mm2 = m2*h2 + m3*l2;
mm3 = m3*h3;
j1 = i1 + m1*h1^2 + m2*l1^2 + m3*l1^2;
j2 = i2 + m2*h2^2 + m3*l2^2;
j3 = i3 + m3*h3^2;
cp1 = cp1p + cd1*k1^2; cp2 = cp2p + cd2*k2^2;
ip1 = ip1p + id1*k1^2; ip2 = ip2p + id2*k2^2;
M = [ j1+ip1     l1*mm2-ip1    l1*mm3
      l1*mm2-ip1 j2+ip1+ip2    l2*mm3-ip2
      l1*mm3     l2*mm3-ip2    j3+ip2];
N = [c1+c2+cp1   -c2-cp1          0
     -c2-cp1     c2+c3+cp1+cp2   -c3-cp2
        0        -c3-cp2          c3+cp2];
P = [-mm1*g     0             0
        0    -mm2*g           0
        0       0          -mm3*g];
GG = [k1  0
     -k1  k2
      0  -k2];
%
% 15% uncertainty in the inertial moments
p1 = 0.15; p2 = 0.15; p3 = 0.15;
```

```
Mp = diag([ i1*p1 i2*p2 i3*p3 ]);
%
% 20% uncertainty in the friction coefficients
s1 = 0.20; s2 = 0.20; s3 = 0.20;
N1 = [c1*s1 -(c2+cp1)*s2       0
        0    (c2+cp1)*s2 -(c3+cp2)*s3
        0         0       (c3+cp2)*s3];
N2 = [ 1  0  0
      -1  1  0
       0 -1  1];
T = [1 -1  0
     0  1 -1
     0  0  1];
%
% construct plant matrices
A = [zeros(3)     eye(3)
     -M\P         -M\N ];
Bj = [zeros(3)
       -M\Mp  ];
Bc = [zeros(3)
       -M\N1  ];
B1 = [Bj Bc];
B2 = [zeros(3) zeros(3,2)
       M\T       -M\GG   ];
B = [B1 B2];
Cj = [-M\P -M\N];
Cc = [zeros(3) N2];
C1 = [Cj
      Cc];
Cy = [1 0 0 0 0 0
      0 1 0 0 0 0
      0 0 1 0 0 0];
Cm = [ alf1    0   0    0   0   0
      -alf2  alf2  0    0   0   0
        0   -alf3 alf3  0   0   0];
C2 = [Cy
      Cm];
C = [C1
     C2];
Djj = -M\Mp;
```

```
Djc = -M\N1;
Dcj = zeros(3);
Dcc = zeros(3);
D11 = [Djj Djc
       Dcj Dcc];
Djt = M\T;
Dju = -M\GG;
Dct = zeros(3);
Dcu = zeros(3,2);
D12 = [Djt Dju
       Dct Dcu];
D21 = [zeros(3) zeros(3)
       zeros(3) zeros(3)];
D22 = [zeros(3) zeros(3,2)
       zeros(3) zeros(3,2)];
D =[D11 D12
    D21 D22];
G = pck(A,B,C,D);
```

Example 2.8 (Disk Drive Servo System)

File: **mod_disk**

```
% Uncertainty model of the Disk Drive Servo System
%
% parameter values
m = 0.2;          % kg
kt = 20.0;        % N/A
ky = 10000.0;     % V/m
kf= 2.51;         % N.s/m
Rcoil = 8;        % Om
Rs = 0.25;        % Om
Rst = 5;          % Om
Rc = Rcoil + Rs; % Om
Lcoil = 0.010;    % H
Lst = 0.002;      % H
Kpa = 11;
%
w1 = 2*pi*70;     z1 = 0.05;    b1 = -0.00575;  b2 = 0.0000115; % w1 =   70 Hz
w2 = 2*pi*2200;   z2 = 0.005;   b3 =  0.0230;   b4 = 0.0;       % w2 = 2200 Hz
w3 = 2*pi*4000;   z3 = 0.05;    b5 =  0.826;    b6 = 0.0;       % w3 = 4000 Hz
w4 = 2*pi*9000;   z4 = 0.005;   b7 =  0.16420;  b8 = 0.0273;    % w4 = 9000 Hz
%
pw1 = 0.05;   pz1 = 0.1;
pw2 = 0.1;    pz2 = 0.4;
pw3 = 0.05;   pz3 = 0.4;
pw4 = 0.05;   pz4 = 0.5;
pkt = 0.1;    pky = 0.05;   pkf = 0.075;
%
% Voice Coil Admittance
tp1 = Lcoil/Rc;
tp2 = Lst/Rst;
tz = (Lcoil + Lst)/Rst;
num_vca = [tz 1];
den_vca = [Rc*tp1*tp2  Rc*tp1+(Rc+Kpa*Rs)*tz  Rc+Kpa*Rs];
Gvca = nd2sys(num_vca,den_vca,Kpa);
%
% Mode 1
A = [ 0     w1
     -w1 -2*w1*z1 ];
```

```
B1 = [ 0   pw1     0
      pw1   0  -2*w1*pz1 ];
B2 = [ 0
       w1];
C1 = [-w1  -2*w1*z1
       0      w1
       0      z1   ];
C2 = [ b1  b2];
D11 = [ 0   0  -2*w1*pz1
        0   0      0
        0   0      0    ];
D12 = [ w1
        0
        0 ];
D21 = [ 0  0  0 ];
D22 = 0;
G1 = pck(A,[B1 B2],[C1;C2],[D11 D12;D21 D22]);
%
% Mode 2
A = [ 0     w2
     -w2 -2*w2*z2 ];
B1 = [ 0   pw2     0
      pw2   0  -2*w2*pz2 ];
B2 = [ 0
       w2 ];
C1 = [-w2  -2*w2*z2
       0      w2
       0      z2   ];
C2 = [ b3  b4 ];
D11 = [ 0   0  -2*w2*pz2
        0   0      0
        0   0      0    ];
D12 = [ w2
        0
        0 ];
D21 = [ 0  0  0 ];
D22 = 0;
G2 = pck(A,[B1 B2],[C1;C2],[D11 D12;D21 D22]);
%
% Mode 3
```

```
A = [ 0     w3
     -w3 -2*w3*z3 ];
B1 = [ 0   pw3     0
      pw3   0  -2*w3*pz3 ];
B2 = [ 0
       w3 ];
C1 = [-w3  -2*w3*z3
       0      w3
       0      z3   ];
C2 = [ b5  b6 ];
D11 = [ 0   0  -2*w3*pz3
        0   0      0
        0   0      0    ];
D12 = [ w3
        0
        0 ];
D21 = [ 0  0  0 ];
D22 = 0;
G3 = pck(A,[B1 B2],[C1;C2],[D11 D12;D21 D22]);
%
% Mode 4
A = [ 0     w4
     -w4 -2*w4*z4 ];
B1 = [ 0   pw4     0
      pw4   0  -2*w4*pz4 ];
B2 = [ 0
       w4 ];
C1 = [-w4  -2*w4*z4
       0      w4
       0      z4   ];
C2 = [ b7  b8 ];
D11 = [ 0   0  -2*w4*pz4
        0   0      0
        0   0      0    ];
D12 = [ w4
        0
        0 ];
D21 = [ 0  0  0 ];
D22 = 0;
G4 = pck(A,[B1 B2],[C1;C2],[D11 D12;D21 D22]);
```

```
%
% Rigid-body plant model
A = [ 0   ky
      0 -kf/m ];
B1 = [  0   pky    0
      pkt/m  0  -pkf/m ];
B2 = [  0
       kt/m ];
C1 = [ 0  0
       0  ky
       0  kf ];
C2 = [ 1  0];
D11 = [ 0 0 0
        0 0 0
        0 0 0 ];
D12 = [ kt
        0
        0];
D21 = [ 0  0  0 ];
D22 = 0;
Grb = pck(A,[B1 B2],[C1;C2],[D11 D12;D21 D22]);
%
% model connection
systemnames = ' Gvca G1 G2 G3 G4 Grb ';
inputvar = '[ pert{15}; control ]';
outputvar = '[ G1(1:3); G2(1:3); G3(1:3); G4(1:3); Grb(1:4) ]';
input_to_Gvca = '[ control ]';
input_to_G1 = '[ pert(1:3);   Gvca ]';
input_to_G2 = '[ pert(4:6);   Gvca ]';
input_to_G3 = '[ pert(7:9);   Gvca ]';
input_to_G4 = '[ pert(10:12); Gvca ]';
input_to_Grb = '[ pert(13:15); G1(4)+G2(4)+G3(4)+G4(4) ]';
sysoutname = 'G';
cleanupsysic = 'yes';
sysic
```